Document made available under the Patent Cooperation Treaty (PCT)

International application number: PCT/US04/021029

International filing date: 30 June 2004 (30.06.2004)

Document type: Certified copy of priority document

Document details: Country/Office: US
Number: 60/483,719
Filing date: 30 June 2003 (30.06.2003)

Date of receipt at the International Bureau: 27 August 2004 (27.08.2004)

Remark: Priority document submitted or transmitted to the International Bureau in compliance with Rule 17.1(a) or (b)

World Intellectual Property Organization (WIPO) - Geneva, Switzerland
Organisation Mondiale de la Propriété Intellectuelle (OMPI) - Genève, Suisse

1212203

THE UNITED STATES OF AMERICA

TO ALL TO WHOM THESE PRESENTS SHALL COME:

UNITED STATES DEPARTMENT OF COMMERCE

United States Patent and Trademark Office

August 16, 2004

THIS IS TO CERTIFY THAT ANNEXED HERETO IS A TRUE COPY FROM THE RECORDS OF THE UNITED STATES PATENT AND TRADEMARK OFFICE OF THOSE PAPERS OF THE BELOW IDENTIFIED PATENT APPLICATION THAT MET THE REQUIREMENTS TO BE GRANTED A FILING DATE.

APPLICATION NUMBER: ***60/483,719***
FILING DATE: ***June 30, 2003***
RELATED PCT APPLICATION NUMBER: ***PCT/US04/21029***

Certified by

Jon W Dudas

Acting Under Secretary of Commerce
for Intellectual Property
and Acting Director of the U.S.
Patent and Trademark Office

Boer 7-3-2-3

IN THE UNITED STATES
PATENT AND TRADEMARK OFFICE

PROVISIONAL APPLICATION

INVENTOR(S)	Bas Driesen Tim Schenk Jan Boer Allert Van Zelst
CASE	Boer 7-3-2-3

"Express Mail" Label No.: EV326908272US
I hereby certify that this paper is being deposited with the United States Postal Service "Express Mail Post Office to Addressee" service under 37 C.F.R. §1.10 on the date indicated below and is addressed to: Commissioner for Patents, P.O. Box 1450, Alexandria, VA 22313-1450

Date of Deposit: June 30, 2003
Signature: Jena Mauro

TITLE MIMO-OFDM Training and Channel Estimation

MAIL STOP PROVISIONAL PATENT APPLICATION
COMMISSIONER FOR PATENTS
P.O. BOX 1450
ALEXANDRIA, VA 22313-1450

PROVISIONAL APPLICATION COVER SHEET

SIR:

This is a request to file a Provisional Application under 37 C.F.R. § 1.53(c). Enclosed herewith are the following:

Specification (including figures embedded in text) – 52 pages

Inventor Residence Information:

Bas Driesen	Breitnerstraat 3, Dongen, Netherlands 5102 EC
Tim Schenk	Frans Halsstraat 26b, Utrecht, Netherlands 3583 BR
Jan Boer	Sint Nicolaaslaan 46, Odijk, Netherlands 3431 JZ
Allert Van Zelst	Paardebloemweide 53, Woerden, Netherlands 3448 TL

Please charge **Deposit Account No. 50-0762** the amount of $160.00, to cover the provisional application filing fee. In the event of non-payment or improper payment of a required fee, the Commissioner is authorized to charge or to credit **Deposit Account No. 50-0762** as required to correct the error. A duplicate copy of this letter is enclosed.

Please address all correspondence to: **Ryan, Mason & Lewis, LLP, 1300 Post Road, Suite 205, Fairfield, CT 06824.** Telephone calls should be made to the undersigned attorney at (203) 255-6560.

Respectfully submitted,

Kevin M. Mason

Kevin M. Mason
Reg. No. 36,597
Attorney for Applicant(s)

Date: June 30, 2003
Ryan, Mason & Lewis, LLP
1300 Post Road, Suite 205
Fairfield, CT 06824

IDR: MIMO-OFDM training and channel estimation

Statement of problem solved by the invention:

Brief problem statement:

A MIMO-OFDM (Multiple Input Multiple Output - Orthogonal Frequency Division Multiplexing) system transmits separate data streams at the same time in space and frequency to achieve a higher throughput. This is achieved by using multiple antennas at both the transmitter and receiver side. To be able to again extract and detect the different data streams, the MIMO-OFDM receiver needs to know the channel matrix **H**, as shown in Figure 1.

Before decoding the data, the MIMO-OFDM receiver needs to acquire the channel matrix **H** through training, just like any other communication systems using coherent detection. This is generally achieved using a specific training signal (preamble), which adds up to the total overhead of the system. The overhead of the system should be kept as low as possible, as it decreases the total throughput of the communication system. Therefore it is important to design a length-efficient training signal. Compared to a conventional SISO (Single Input Single Output) system a MIMO-OFDM system needs to estimate many more channels ($N_t N_r$ times more), making efficient training even more important. The challenge is now to keep the training length limited or preferably equal to a SISO system.

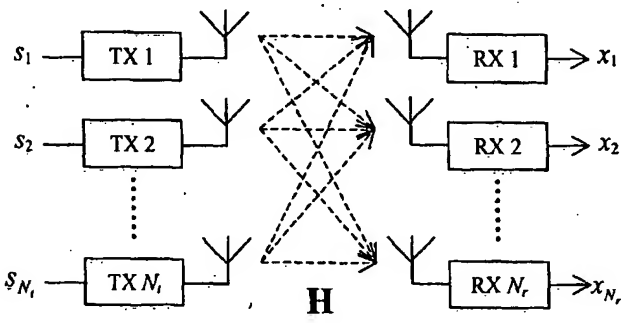

Figure 1: MIMO system, consisting of N_t transmitters and N_r receivers, and channel matrix H

Prior design / purposes and advantages:

A lot of knowledge on efficient channel training for OFDM can be found in the literature and some are already standardized, for example the preamble for IEEE 802.11a/g systems [1]. A lot of research has been done on efficient channel training for MIMO systems and MIMO-OFDM systems. It is known that the most efficient training of a MIMO-OFDM system is a signal that is orthogonal in frequency domain or equally shift orthogonal in time domain. In time domain it can be intuitively understood as, when the training signal would not be orthogonal then the CSI (Channel State Information) for a single path cannot be separated from the other paths. Furthermore, when the training signal would not be shift orthogonal then also the CSI of single path cannot be correctly obtained because the delayed training

signals of the other paths are not orthogonal to this one. Delayed versions of the training signal are received because of multipath, which is caused by reflections in the environment. The following focuses on a MIMO-OFDM system specifically designed for WLAN systems, but it must be understood that other applications could use a similar approach.

The IEEE specified a preamble in frequency domain for 802.11a/g OFDM based WLAN systems [1], consisting of short and long training symbols. The short training symbols are for frame detection, setting the AGC and coarse synchronization. The long training symbols are used for fine synchronization and channel estimation. In the frequency domain the long training symbol according the IEEE is specified as follows

$$\mathbf{t}_l = [0\,1\,-1\,-1\,1\,1\,-1\,1\,-1\,1\,-1\,-1\,-1\,-1\,1\,1\,-1\,1\,-1\,1\,1\,1\,1\,0\cdots$$
$$\cdots 0\,1\,1\,-1\,-1\,1\,1\,-1\,1\,1\,1\,1\,1\,1\,-1\,-1\,1\,1\,-1\,1\,1\,1\,1\,1]$$

which consists of 64 subcarriers of which 52 are modulated. It can be modified to accommodate channel estimation for a MIMO-OFDM system. As mentioned before the ideal training for a MIMO-OFDM system is orthogonal in frequency domain or again equally shift orthogonal in time domain. The IEEE 802.11a/g long training symbol can be made orthogonal when diagonally loading the modulated subcarriers on the different transmit antennas. For a three transmit antenna MIMO-OFDM systems this would look, for the first 16 subcarriers like

$$\begin{aligned}
\mathbf{t}_l^1 &= [0\ \ 1\ \ 0\ \ 0\ \ 1\ \ 0\ \ 0\ \ 1\ \ 0\ \ 0\ \ -1\ \ 0\ \ 0\ \ -1\ \ 0\ \cdots \\
\mathbf{t}_l^2 &= [0\ \ 0\ \ -1\ \ 0\ \ 0\ \ 1\ \ 0\ \ 0\ \ -1\ \ 0\ \ 0\ \ -1\ \ 0\ \ 0\ \ -1\ \cdots \\
\mathbf{t}_l^3 &= [0\ \ 0\ \ 0\ \ -1\ \ 0\ \ 0\ \ -1\ \ 0\ \ 0\ \ 1\ \ 0\ \ 0\ \ -1\ \ 0\ \ 0\ \cdots
\end{aligned}$$

where $\mathbf{t}_l^n$ stands for the long training symbol transmitted on the n-th transmit antenna. In this case, on each antenna only one-third of the subcarriers are transmitted. Channel estimation at the receiver side should now use a form of interpolation to find the channel estimate belonging to the nulled subcarriers of a specific transmit antenna. As long as the rms time delay spread (TDS) of the channel is limited or equally the coherence bandwidth is larger than a certain number, the channel estimation error due to interpolation will be small in general.
A problem with this method is that the outer subcarriers of the spectrum do not have neighbour subcarriers and therefore when nulled they cannot be interpolated but need to be extrapolated. Extrapolation creates larger errors than interpolation and a larger error in the channel estimation of the outer subcarriers is unwanted. Furthermore, a MIMO-OFDM system preferably needs to be backwards compatible to the current IEEE 802.11a/g standards, which is a subject that is not explored until now.

Description of the invention:

Suggested is a diagonally loaded long training symbol, based on the IEEE 802.11a-training symbol in frequency domain, with additional subcarriers at the spectrum's edges. As the IEEE 802.11a training only utilizes 52 out of the 64 subcarriers some room is left to specify additional subcarriers. Addition of 4 extra training subcarriers, 2 at each side of the spectrum, is shown to be still in line with the IEEE 802.11a

transmit mask, see the Appendix, Chapter 4. A MIMO-OFDM system with two transmit antennas needs 2 extra subcarriers, one at each side of the spectrum and a MIMO-OFDM system with three transmit antennas needs 4 extra subcarriers, two at each side of the spectrum. The additional subcarriers at edge of the spectrum overcome the problem of the outer subcarriers, as stated in the previous paragraph, as now an interpolation based estimation technique can be used. Figure 2 gives a schematic representation of the MIMO-OFDM long training symbols for a 3 transmit antenna system, with additional subcarriers at the spectrum's edges. The extra subcarriers at the edges (red) are modulated in such a way that the peak-to-average power ratio (PAP) is lowest. Simulation results are given in the Appendix, Chapter 4.

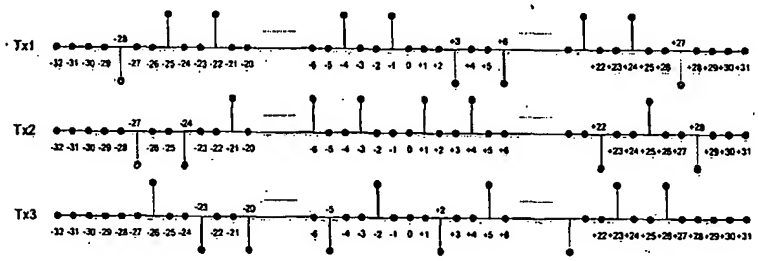

Figure 2: Frequency domain representation of the MIMO-OFDM long training symbols for a 3 transmit antenna system, with 4 added subcarriers at the spectrum's edges.

The optimal solution for a 3 transmit antenna MIMO-OFDM system would include 4 additional subcarriers (2 on each side of the spectrum) to be able to make an accurate estimation of the outer subcarriers. The first long training symbols and the second long training symbols of each antenna would in this case be identical. A sub-optimal solution would be using just 2 additional subcarriers, but interchanging them at the first and the second long training symbols in the way depicted in Figure 3. Where the first long training symbols antenna uses the red marked outer subcarriers and the second long training symbols uses the shaded red marked outer subcarriers.

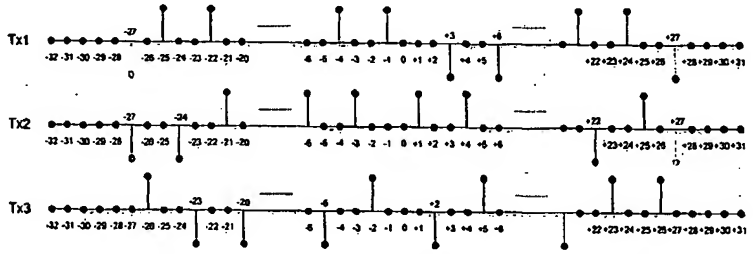

Figure 3: Frequency domain representation of the MIMO-OFDM long training symbols for a 3 transmit antenna system, with 2 added subcarriers at the spectrum's edges.

The preamble can be made backwards compatible with current 802.11a/g based systems. In order to be backwards compatible, 11a/g based systems needs to be able to detect the preamble and interpret the packet's SIGNAL-field. Diagonally loading of the SIGNAL-field on the different transmit antennas achieves this. The length specified in the SIGNAL-field for a MIMO transmission should be made equal to the actual duration of the packet, so that an 802.11a/g based system could then defer for the duration of the MIMO transmission. A MIMO system needs to be able to translate this into the actual length of the packet in bytes. For this a MIMO system has to have

additional information, which can be included in the reserved bit in the SIGNAL-field, see [1], and in the additional subcarriers when the SIGNAL-field is also appended with extra subcarriers. Furthermore a MIMO-OFDM system based on diagonally loaded long training symbols and SIGNAL-field can be made scalable to different MIMO configurations. For example, a MIMO-OFDM system with three transmit antennas can easily be scaled back to a MIMO-OFDM system with two transmit antennas. Additionally a MIMO-OFDM system with only two receive antennas can train the channel and interpret the SIGNAL-field of a MIMO-OFDM transmission with 3 transmit antennas, and therefore is able to defer for the duration of the packet. A MIMO-OFDM system is then coexistent with 802.11a/g systems and lower order MIMO-OFDM systems. With coexistence is meant, any system with N_r receive antennas that is not able to receive the data transmitted, is able to defer for the duration of the transmission, because it is able to detect the start of the transmission and retrieve the length (duration) of this transmission. Furthermore a MIMO-OFDM system is able to communicate in a backwards-compatible way to an 802.11a/g system in two ways. First of all the data can be diagonally loaded on the different antennas as well and secondly, it is possible to scale back to one antenna. The IEEE 802.11a/g and MIMO-OFDM preamble can be schematically represented as in Figure 4 and Figure 5 respectively. More details can be found in the Appendix, Chapter 6.

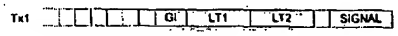

Figure 4: IEEE 802.11a/g preamble structure.

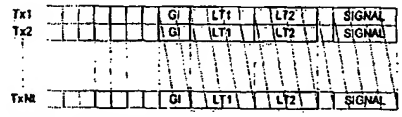

Figure 5: MIMO-OFDM preamble structure.

A diagonally loaded SIGNAL-field has another benefit, namely it can be used to serve as a third long training symbol. The SIGNAL-field is always modulated and encoded in the same robust way, which facilitates good reception. The SIGNAL-field in a MIMO transmission is even more robust, while the SIGNAL-field is received by multiple antennas and thus can be combined in an optimal way. Using the SIGNAL-field as a third long training symbol is therefore a feasible solution, since the chance of a good reception is very high.

Furthermore it is shown in the Appendix, Chapter 7 that shift-diagonally loading the training symbols and SIGNAL-field yields the best performance. However this performance gain can only be achieved at the expense of backwards compatibility and scalability. With shift-diagonally loaded training symbols the inherent interpolation error becomes smaller when each symbol is first processed separately and afterwards combined.

Backwards-compatible channel estimation with equally diagonally loaded training symbols and SIGNAL-field requires the following steps at each receiver:

1. Adding two long training symbols to gain in SNR
2. Transforming the resulting long training symbol to frequency domain

3. Demodulation of the long training symbol, resulting in the incomplete channel estimates.
4. Transforming the SIGNAL-field to frequency domain
5. Detection and decoding of the SIGNAL-field using the incomplete channel estimates
6. Demodulation of the SIGNAL-field, gives another estimate of the incomplete channels
7. Summing and scaling the demodulated SIGNAL-field to the demodulated training symbol (adding up the incomplete channel estimates)
8. Compute the complete channel estimations through interpolation between the known subcarriers.

Non backwards-compatible channel estimation with shift-diagonally loaded training symbols and SIGNAL-field requires the following steps at each receiver:

1. Transforming the long training symbols and SIGNAL-field to frequency domain
2. Demodulate the long training symbols
3. Separate interpolation of the long training symbols
4. Summation and scaling of the interpolated long training symbols
5. Detection and decoding of the SIGNAL-field
6. Demodulation of the SIGNAL-field
7. Interpolation of the SIGNAL-field
8. Update channel estimates through combining interpolated SIGNAL-field and training symbols

Channel estimation is done at the MIMO-OFDM receiver side and takes place after timing and frequency synchronization. Figure 6 gives a block diagram of the MIMO-OFDM receiver and shows the position where the channel estimation takes place.

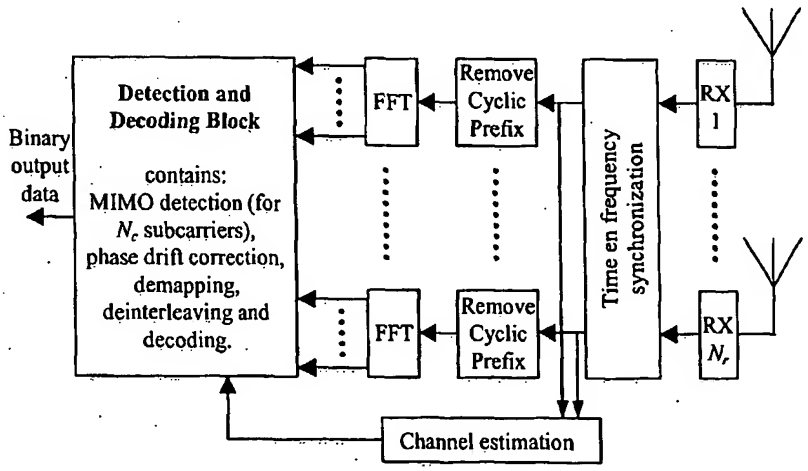

Figure 6: Position in the MIMO-OFDM receiver where channel estimation takes place

With diagonally loaded long training symbols and SIGNAL-field a 3x3 MIMO-OFDM can be realised. When going to higher order MIMO-OFDM systems extra training needs to be included to make accurate channel estimation possible. A rule of thumb is one additional training symbol for one additional transmit antenna. A 5x5 MIMO system would require 4 long training symbols and a SIGNAL-field. The

channels belonging to the first 3 transmitters are estimated with the first two long training symbols and the SIGNAL-field and the channels corresponding to the last 2 transmitters are estimated with the last two long training symbols. Figure 7 is a schematic representation of a preamble structure for such a system.

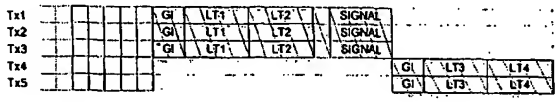

Figure 7: MIMO-OFDM preamble structure for a system with 5 transmit antennas

Summary of Invention

Key inventive concepts:

- A MIMO-OFDM system that is coexistent and backwards-compatible to lower order MIMO-OFDM systems and current IEEE 802.11a/g systems
- Diagonally loaded training and SIGNAL-field, which achieves a MIMO-OFDM preamble up to three transmit antennas that has equal length to current IEEE 802.11a/g OFDM systems
- Diagonally loaded SIGNAL-field used as a third long trainings symbol
- The proposed MIMO-OFDM preamble is backwards compatible with current IEEE 802.11a/g systems and is scalable to other MIMO configurations
- Shift-diagonally loading the training symbols and the SIGNAL-field on the transmit antennas leads to more accurate channel estimates, but removes backwards compatibility
- Addition of extra subcarriers at the spectrum's edges improves the channel estimate at the outer subcarriers and moreover can be used to include additional information for specifying a MIMO-OFDM system
- Channel estimation procedure
- Training and channel estimation concept can be extended to MIMO-OFDM systems with more than 3 transmit antennas.

Reference:

[1] IEEE Std 802.11a-1999, "*Part 11: Wireless LAN medium access control (MAC) and physical layer (PHY) specification: high-speed physical layer in the 5 GHz band*".

Appendix: MIMO-OFDM channel estimation

MIMO-OFDM Channel Estimation

by Bas Driesen, April 18th 2003

agere systems

Table of Contents:

1 Introduction

Existing WLAN systems based upon OFDM modulation are in compliance with the IEEE 802.11a/g standard and are said to provide up to 54 Mb/s. Although theoretically being able to provide 54 Mb/s in practice this is most of the times difficult to achieve, especially when a wide coverage is demanded. Furthermore the need already exists to have even higher data rates available, to support for example multiple high-definition television channels. Accordingly the key objectives of next generation WLAN systems are more robustness and more capacity.

Although the above stated objectives can be obtained in a number of different ways, the use of multiple transmit and receive antennas has been identified as a very promising solution to achieve more robustness as well as more capacity. More robustness can easily be achieved through different kind of techniques that exploit the spatial diversity and additional gain introduced in the system with more antennas [19]. More capacity can be achieved in multipath fading environments with very bandwidth efficient MIMO techniques [17], [18].

MIMO systems transmit separate data streams on a number of transmit antennas and receive a combination of these data streams on a number of receive antennas. The difficulty is now to distinguish between the different data streams at the receiver side. All kind of MIMO decoding techniques are known, but all of them rely on the availability of accurate channel estimations [20], [21].

This document investigates and compares a number of feasible channel estimation techniques for a MIMO OFDM system. An extra difficulty is that these techniques should be applicable in real-life systems and should ideally be backwards compatible with current systems. First of all, Chapter 2 addresses the different training techniques, after which Chapter 3 describes the accompanying channel estimation realizations. Chapter 4 then elaborates on two key problems. The PAP-ratios of the training sequences are listed in Chapter 5. Next Chapter 6 looks into backwards compatibility and scalability. Finally Chapter 7 gives performance results and Chapter 8 gives the conclusions and recommendations.

Intentionally Blank.
KMA

2 Training Techniques

Current SISO-OFDM systems based on the IEEE 802.11a standard use a preamble for synchronization and channel estimation [11]. This preamble is built out of short and long training sequences. The long training sequences are merely used for channel estimation. The format of the IEEE 802.11a short and long training sequence in frequency domain is given below

$$\mathbf{t}_s = \sqrt{13/6}\,[0000(-1-j)000(-1-j)000(1+j)000(1+j)000(1+j)000(1+j)00\cdots$$

$$\cdots 00(1+j)000(-1-j)000(1+j)000(-1-j)000(-1-j)000(1+j)0000]$$

$$\mathbf{t}_l = [01-1-111-11-11-1-1-1-1-111-1-11-11-111110\cdots$$
$$\cdots 011-1-111-11-1111111-1-111-11-11111] \tag{2.1}$$

A long training symbol consists out of 52 modulated subcarriers, notice that the 0Hz (DC) subcarrier is zero. In time domain two of these long training sequences are concatenated and are preceded by a guard interval, which is a periodical extension of the long training sequence. In formula form expressed as

$$\tilde{t}_l(k-N/2) = \sum_{n=0}^{n=N-1} t_l(n) e^{j\frac{2\pi}{N}n(k-N/2)} \qquad \text{for} \qquad k=0\cdots 2N+N/2-1 \tag{2.2}$$

with N equal to 64 and ~ denotes the time domain representative. The short training sequence can be expressed in similar form

$$\tilde{t}_s(k) = \sum_{n=0}^{n=N-1} t_s(n) e^{j\frac{2\pi}{N}nk} \qquad \text{for} \qquad k=0\cdots 2N+N/2-1. \tag{2.3}$$

The total preamble excluding windowing then becomes

$$\tilde{t}_t(k) = \tilde{t}_s(k) + \tilde{t}_l(k-N/2-(2N+N/2-1)) \qquad \text{for} \qquad k=0\cdots 5N-1 \tag{2.4}$$

and looks like Figure 1.

The equivalent in matrix notation is

$$\tilde{\mathbf{t}}_s = \mathbf{t}_s \mathbf{F}_N^{-1}\begin{pmatrix} \mathbf{0} & \mathbf{I}_N & \mathbf{I}_N \\ \mathbf{I}_{N/2} & & \end{pmatrix}, \quad \tilde{\mathbf{t}}_l = \mathbf{t}_l \mathbf{F}_N^{-1}\begin{pmatrix} \mathbf{0} & \mathbf{I}_N & \mathbf{I}_N \\ \mathbf{I}_{N/2} & & \end{pmatrix}, \quad \tilde{\mathbf{t}}_t = [\tilde{\mathbf{t}}_s \quad \tilde{\mathbf{t}}_l] \tag{2.5}$$

where

$$\mathbf{F}_N = \begin{bmatrix} W_N^0 & W_N^0 & W_N^0 & \cdots & W_N^0 \\ W_N^0 & W_N^1 & W_N^2 & \cdots & W_N^{N-1} \\ W_N^0 & W_N^2 & W_N^4 & \cdots & W_N^{2(N-1)} \\ \vdots & \vdots & \vdots & \ddots & \vdots \\ W_N^0 & W_N^{N-1} & W_N^{2(N-1)} & \cdots & W_N^{(N-1)^2} \end{bmatrix} \qquad \text{with} \qquad W_N^k = e^{-j\frac{2\pi}{N}k}. \tag{2.6}$$

$\mathbf{F}_N$ is the $N \times N$ Fourier matrix and $\mathbf{I}_N$ is the identity matrix of size N, furthermore the index l represents the long training sequence and is used to identify the inner

matrix dimensions. A bold letter denotes a vector, a bold capital letter denotes a matrix and normal letter represents a singleton dimension.

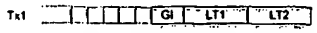

Figure 1: Short and long training sequences extended with guard interval

2.1 Repetition

The first MIMO-OFDM training technique evaluated is actually a very simple one, namely it is based on a repetition of the standard IEEE 802.11a training sequence. For every transmit antenna two long training symbols including guard interval are sent out subsequently in time, meaning first antenna one sends out the training, then antenna two and so on. In this case the overhead grows linearly with the number of transmit antennas, which is actually not desirable, because it reduces the throughput of the system.

The format of the training sequences is the same as previously described, with the difference that

$$\begin{aligned} \tilde{\mathbf{t}}_t &= \left[\tilde{t}_1 \quad \cdots \quad \tilde{t}_1\right]^T && N_t \times \left(\frac{1}{2}N + 2N\right) \\ \tilde{\mathbf{T}}_1 &= \mathbf{I}_{N_t} \otimes \mathbf{t}_f \mathbf{F}_N^{-1} \begin{pmatrix} \mathbf{0} & \mathbf{I}_N & \mathbf{I}_N \\ \mathbf{I}_{N/2} & & \end{pmatrix} && N_t \times N_t \left(\frac{1}{2}N + 2N\right) \\ \tilde{\mathbf{T}}_t &= \left[\tilde{\mathbf{t}}_1 \quad \tilde{\mathbf{T}}_1\right] && N_t \times (N_t + 1)\left(\frac{1}{2}N + 2N\right) \end{aligned} \tag{2.7}$$

where $\otimes$ is the Kronecker product and $\tilde{\mathbf{T}}_t$ stands for the total training. Figure 2 gives a schematic representation.

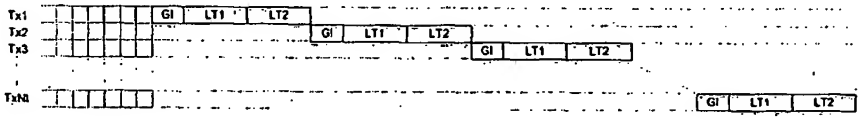

Figure 2: Repetition of the training sequences

2.2 Subcarrier Orthogonal

It is shown that the ideal training sequences in a MIMO-OFDM transceiver are constant modulus and subcarrier orthogonal in frequency domain or equally shift orthogonal in time domain [1], [8], [5], [4], [6]. In time domain it can be intuitively understood as, when the training sequences would not be orthogonal then the CSI (Channel State Information) for a single path cannot be separated from the other paths and when the training sequence would not be cyclic orthogonal then also the CSI of single path cannot be correctly obtained because the delayed versions of the other training sequences are not orthogonal to this one.

The 802.11a constant modulus long training sequence can be made orthogonal in the following way

$$\mathbf{t}_t = \begin{pmatrix} \mathbf{t}_t\Omega_{N,1} \\ \vdots \\ \mathbf{t}_t\Omega_{N,N_t} \end{pmatrix} \qquad N_t \times N \qquad (2.8)$$

with $\Omega_{N,x}$ a diagonal matrix of size N creating orthogonal training sequences. Several $\Omega_{N,x}$ exist that satisfy the orthogonality constraint. A possible choice would be

$$\Omega_{N,x} = diag\left(0_x \quad 1 \quad 0_{N_t-1} \quad \cdots \quad \cdots \quad 0_{N_t-1} \quad 1 \quad 0_{N_t-1-x}\right) \qquad N \times N \qquad (2.9)$$

where 0_x this time is a row vector with length x. Another choice would be

$$\Omega_{N,x} = diag\left(0 \quad \mathbf{f}_{p,(N_{sc}/2+1:N_{sc})} \quad 0 \quad \cdots \quad 0 \quad \mathbf{f}_{p,(1:N_{sc}/2)}\right) \qquad N \times N \qquad (2.10)$$

with $\mathbf{f}_{p,(l:k)}$ the l till k-th elements of p-th column vector of the Fourier matrix $\mathbf{F}_N$, $p = 1 + (x-1)\lfloor N/N_t \rfloor$ and N_{sc} is equal to the number of used subcarriers. From this point of on the training sequence that uses (2.9) is called the diagonally loaded training sequence and the training sequence that uses (2.10) is called the Fourier training sequence.

The actual preamble in time domain then becomes

$$\begin{aligned} \tilde{\mathbf{t}}_s &= \left[\tilde{t}_s \quad \cdots \quad \tilde{t}_s\right]^T && N_t \times \left(\frac{1}{2}N + 2N\right) \\ \tilde{\mathbf{t}}_l &= \mathbf{t}_t \mathbf{F}_N^{-1} \begin{pmatrix} 0 & & \\ I_{N/2} & I_N & I_N \end{pmatrix} && N_t \times \left(\frac{1}{2}N + 2N\right) \\ \tilde{\mathbf{T}}_t &= \left[\tilde{\mathbf{t}}_s \quad \tilde{\mathbf{t}}_l\right] && N_t \times 5N \end{aligned} \qquad (2.11)$$

which has the same length as the original 802.11a preamble. Figure 3 gives a schematic representation.

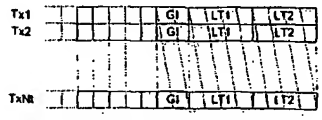

Figure 3: Subcarrier orthogonal long training sequences

2.3 Single Carrier

Previously a shift-orthogonal training sequence in time domain was developed [2]. This training sequence is called the single carrier training sequence and is based on phase-shift pulse codes that have ideal correlation properties [16], [15]. The training sequence is constructed using the size M Fourier matrix and concatenating all rows to obtain a $M^2 = N$ long training sequence

$$\tilde{\mathbf{t}}_l = \left[W^0 \quad \cdots \quad W^0 \quad W^0 \quad \cdots \quad W^{M-1} \quad W^0 \quad \cdots \quad W^{2(M-1)} \quad \cdots \quad W^0 \quad \cdots \quad W^{(M-1)^2}\right] \qquad (2.12)$$

Below it is shown that this training sequence has ideal correlation properties, meaning that this training sequence only shows a peak when correlated with an exact copy and results in zero when correlated with shifted versions of itself.

$$\phi(d) = \sum_{k=0}^{M^2-1} t_l(k+d)t_l^*(k) \qquad \text{for} \quad d = 0 \cdots M^2 - 1 \tag{2.13}$$

$$= \sum_{i=0}^{M-1} \sum_{k=iM}^{iM+M-1} t_l(k+d)t_l^*(k) = \sum_{i=0}^{M-1} \sum_{r=0}^{M-1} t_l(r+iM+d)t_l^*(r+iM)$$

If d is now split in the same way as k the correlation can be written as

$$\phi(x+pM) = \sum_{i=0}^{M-1} \sum_{r=0}^{M-1} t_l(r+iM+x+pM)t_l^*(r+iM) = \sum_{l=0}^{M-1} \sum_{r=0}^{M-1} W_M^{(r+x)(i+p)} W_M^{-ri} \tag{2.14}$$

$$= \sum_{i=0}^{M-1} W_M^{xi} \sum_{r=0}^{M-1} W_M^{p(r+x)} = M^2 \qquad \text{for} \quad p = 0 \;\; \& \;\; x = 0$$

$$\text{else} \quad 0$$

which proves the ideal correlation property.

Transformation of single carrier training sequence to frequency domain gives

$$T_l(n) = \sum_{k=0}^{N-1} t_l(k) W_N^{kn} \tag{2.15}$$

$$= \sum_{i=0}^{M-1} \sum_{k=iM}^{iM+M-1} t_l(k) W_N^{kn} = \sum_{i=0}^{M-1} \sum_{k=0}^{M-1} t_l(k+iM) W_N^{(k+iM)n} = \sum_{i=0}^{M-1} \sum_{k=0}^{M-1} W_M^{ki} W_N^{(k+iM)n}$$

$$= \sum_{k=0}^{M-1} W_N^{kn} \sum_{i=0}^{M-1} W_M^{i(k+n)} = M W_N^{(M-n)n} \qquad \text{for} \quad n = 0 \cdots N-1$$

which shows that the frequency domain signal has a constant amplitude and a changing phase. Furthermore it can be seen that shifting the single carrier sequence in time results in orthogonal sequences in frequency domain. From these observations it can be concluded that the single carrier training sequence actually belongs to the same category as the subcarrier orthogonal training sequences. In vector format the normalized single carrier training sequence with time-shift k is expressed in frequency domain as

$$\omega_k = \left[W_N^0 \quad W_N^{(M-1)+k} \quad W_N^{2(M-2)+2k} \quad W_N^{3(M-3)+3k} \quad \cdots \quad W_N^{(N-1)(M-(N-1))+(N-1)k} \right] \tag{2.16}$$

A similar orthogonality rule as in Chapter 2.2 can now be constructed as

$$\Omega_{N,x} = diag\left(0 \quad \omega_{p,(N_{sc}/2+1:N_{sc})} \quad 0 \quad \cdots \quad 0 \quad \omega_{p,(1:N_{sc}/2)}\right) \tag{2.17}$$

with $p = (x-1)\lfloor N / N_t \rfloor$. In this way the single carrier training sequence can be treated the same as the subcarrier orthogonal training sequences.

3 Channel Estimation

The channel estimation in the receiver of an IEEE 802.11a/g system uses the long training sequences described in the previous chapter. The received long training signal can be written as

$$\tilde{r}_l(k-N/2)=\tilde{t}_l(k-N/2)*\tilde{h}(k)+ \tilde{t}_s\left(k+\frac{1}{2}N+2N\right)*\tilde{h}(k)+\tilde{v}(k-N/2) \quad \text{for} \quad k=0\cdots 2N+N/2-1 \tag{3.1}$$

where $\tilde{r}_l(k)$ is the received signal, $\tilde{t}_l(k)$ the long training sequence as specified in (2.1), $\tilde{h}(k)$ is the channel impulse response and $\tilde{v}(k)$ is the additive Gaussian noise.

At the receiver first the guard interval is removed and then the two of the long training sequences are added to get a 3 dB gain in SNR, which result in

$$\tilde{r}_l(k)+\tilde{r}_l(k+N)=2\tilde{t}_l(k)*\tilde{h}(k)+\tilde{v}(k)+\tilde{v}(k+N) \quad \text{for} \quad k=0\cdots N-1$$
$$E\left\{\left|\tilde{r}_l(k)+\tilde{r}_l(k+N)\right|^2\right\}=4\sigma_s^2+2\sigma_v^2 \tag{3.2}$$

when $\tilde{h}(k)$ has a length smaller than the guard interval of the long training sequences and where σ_s^2 is the variance of the long training symbol convolved with the channel. After that the resulting training sequence is transformed to frequency domain,

$$r_l(n)=2t_l(n)h(n)+w(n) \quad \text{for} \quad n=0\cdots N-1. \tag{3.3}$$

where $w(n)$ is the resulting frequency domain noise component. Each subcarrier is then demodulated with its respective reference counterpart, which leads to a channel estimation per subcarrier in frequency domain

$$h_{est}(n)=\frac{1}{2}t_l(n)^* r_l(n)=h(n)+\frac{1}{2}t_l(n)^* w(n) \quad \text{for} \quad n=0\cdots N-1. \tag{3.4}$$

when $|t_l(n)|^2=1$ for all non-zero subcarriers, which is true.

The equivalent in matrix notation is

$$\tilde{\mathbf{r}}_l=\tilde{\mathbf{t}}_l\tilde{\mathbf{H}}_l+\tilde{\mathbf{t}}_s\tilde{\mathbf{H}}_s+\tilde{\mathbf{v}}_l \quad ,1\times\left(\frac{1}{2}N+2N\right) \tag{3.5}$$

where

$$\tilde{\mathbf{H}}_l = \begin{pmatrix} h(0) & \cdots & h(\Gamma-1) & 0 & \cdots & 0 \\ 0 & \ddots & & \ddots & \ddots & \vdots \\ \vdots & \ddots & \ddots & & \ddots & 0 \\ \vdots & & \ddots & \ddots & & h(\Gamma-1) \\ \vdots & & & \ddots & \ddots & \vdots \\ 0 & \cdots & \cdots & \cdots & 0 & h(0) \end{pmatrix} \quad ,\left(\frac{1}{2}N+2N\right)\times\left(\frac{1}{2}N+2N\right) \tag{3.6}$$

with Γ the length of the channel and $\tilde{\mathbf{H}}_s$ is a matrix with all elements equal to zero, except for the elements in the lower left corner, which are defined as

$$\begin{pmatrix} h(1) & & 0 \\ \vdots & \ddots & \\ h(\Gamma-1) & \cdots & h(1) \end{pmatrix} \tag{3.7}$$

finally $\tilde{\mathbf{v}}_l$ stands for the time domain noise vector.

Removing the guard interval and adding the two long training sequences results in

$$\tilde{\mathbf{y}} = \tilde{\mathbf{r}}_l(0 \quad \mathbf{I}_N \quad 0)^T + \tilde{\mathbf{r}}_l(0 \quad 0 \quad \mathbf{I}_N)^T = 2\mathbf{t}_l\mathbf{F}_N^{-1}\tilde{\mathbf{H}}_l' + \tilde{\mathbf{w}}_l \quad ,1\times N \tag{3.8}$$

where

$$\tilde{\mathbf{H}}_l' = \begin{pmatrix} h(0) & \cdots & h(\Gamma-1) & & 0 \\ & \ddots & & \ddots & \\ & & \ddots & & \ddots \\ h(\Gamma-1) & & 0 & \ddots & h(\Gamma-1) \\ \vdots & \ddots & & \ddots & \vdots \\ h(1) & \cdots & h(\Gamma-1) & & h(0) \end{pmatrix} \quad ,N\times N \tag{3.9}$$

and $\tilde{\mathbf{w}}_l$ is the resulting noise vector.

Transformation to frequency domain gives

$$\mathbf{x} = \tilde{\mathbf{y}}\mathbf{F}_N = 2\tilde{\mathbf{t}}_l\mathbf{F}_N^{-1}\tilde{\mathbf{H}}_l'\mathbf{F}_N + \tilde{\mathbf{w}}_l\mathbf{F}_N = 2\mathbf{t}_l\mathbf{H}_l + \mathbf{w}_l \quad ,1\times N \tag{3.10}$$

with

$$\mathbf{H}_l = \begin{pmatrix} H(0) & & 0 \\ & \ddots & \\ 0 & & H(N-1) \end{pmatrix} \quad ,N\times N \tag{3.11}$$

Representing the N frequency bins of the channel.

The frequency domain channel estimate is found by demodulation with the original training sequence

$$\mathbf{h}_{est,l} = \frac{1}{2}\mathbf{t}_l^*\mathbf{X} = \mathbf{h}_l + \frac{1}{2}\mathbf{t}_l^*\mathbf{W}_l \quad \text{with } \mathbf{X} = \text{diag}(\mathbf{x}) \text{ and } \mathbf{W} = \text{diag}(\mathbf{w}) \tag{3.12}$$

3.1 Repetition

Estimating the channel in the repetition case goes the same as in the SISO-OFDM case and mathematically it can be written as

$$\tilde{\mathbf{R}}_l = \tilde{\mathbf{T}}_l \tilde{\mathbf{H}}_L + diag(\tilde{\mathbf{t}}_l)\tilde{\mathbf{H}}_S + \tilde{\mathbf{N}}_l \qquad , N_t \times N_r\left(\frac{1}{2}N + 2N\right) \tag{3.13}$$

where

$$\tilde{\mathbf{H}}_L = \begin{pmatrix} \tilde{\mathbf{H}}_l^{11} & \cdots & \tilde{\mathbf{H}}_l^{1N_r} \\ \vdots & \ddots & \vdots \\ \tilde{\mathbf{H}}_l^{N_t 1} & \cdots & \tilde{\mathbf{H}}_l^{N_t N_r} \end{pmatrix} \qquad , N_t\left(\frac{1}{2}N + 2N\right) \times N_r\left(\frac{1}{2}N + 2N\right) \tag{3.14}$$

with $\tilde{\mathbf{H}}_l^{xy}$ given by (3.6), the upper indices specify different elements of the channel across the antennas and $\tilde{\mathbf{N}}_l$ represents the noise matrix.

Removing again the guard interval and adding the two training symbols gives

$$\begin{aligned} \tilde{\mathbf{Y}}_l &= \tilde{\mathbf{R}}_l\left(\mathbf{1}_{N_r} \otimes (\mathbf{0}_{N/2} \quad \mathbf{I}_N \quad \mathbf{0}_N)^T\right) + \tilde{\mathbf{R}}_l\left(\mathbf{1}_{N_r} \otimes (\mathbf{0}_{N/2} \quad \mathbf{0}_N \quad \mathbf{I}_N)^T\right) \\ &= 2\left(\mathbf{I}_{N_t} \otimes \mathbf{t}_l \mathbf{F}_N^{-1}\right)\tilde{\mathbf{H}}_L' + \tilde{\mathbf{W}}_l \qquad , N_t \times N_r N \end{aligned} \tag{3.15}$$

where $\mathbf{1}_{N_r}$ stands for an all-one matrix of size N_r, $\tilde{\mathbf{H}}_L'$ is the same as $\tilde{\mathbf{H}}_L$, only with its elements equal to $\tilde{\mathbf{H}}_l'^{xy}$.

Transformation to frequency domain gives

$$\begin{aligned} \mathbf{X}_l &= \tilde{\mathbf{Y}}_l\left(\mathbf{1}_{N_r} \otimes \mathbf{F}_N\right) = 2\left(\mathbf{I}_{N_t} \otimes \mathbf{t}_l \mathbf{F}_N^{-1}\right)\tilde{\mathbf{H}}_L'\left(\mathbf{1}_{N_r} \otimes \mathbf{F}_N\right) + \tilde{\mathbf{W}}_l\left(\mathbf{1}_{N_r} \otimes \mathbf{F}_N\right) \\ &= 2\left(\mathbf{1}_{N_t} \otimes \mathbf{t}_l\right)\mathbf{H}_L + \mathbf{W}_l \qquad , N_t \times N_r N \end{aligned} \tag{3.16}$$

with $\mathbf{H}_L$ the same structure as $\tilde{\mathbf{H}}_L$, only with its elements equal to $\mathbf{H}_l^{xy}$.

The channel estimation matrix is found by demodulation

$$\mathbf{H}_{est,l} = \frac{1}{2}\left(\mathbf{1}_{N_t} \otimes \mathbf{t}_l^*\right)\mathbf{X}_L = \mathbf{H}_l + \frac{1}{2}\left(\mathbf{1}_{N_t} \otimes \mathbf{t}_l^*\right)\mathbf{W}_L \qquad , N_t \times N_r N \tag{3.17}$$

with $\mathbf{L} = \mathrm{diag}(\mathbf{l})$

3.2 Subcarrier Orthogonal

Estimating the channel when subcarrier orthogonal training sequences are used is similar to the repetition case

$$\tilde{\mathbf{R}}_l = diag(\tilde{\mathbf{t}}_l)\tilde{\mathbf{H}}_L + diag(\tilde{\mathbf{t}}_s)\tilde{\mathbf{H}}_S + \tilde{\mathbf{N}}_l \qquad , N_t \times N_r\left(\frac{1}{2}N + 2N\right) \tag{3.18}$$

with $\tilde{\mathbf{H}}_L$ given in (3.14).

Removing the guard interval and adding the two training symbols gives

$$\tilde{\mathbf{Y}}_l = \tilde{\mathbf{R}}_l\left(\mathbf{1}_{N_r} \otimes (\mathbf{0}_{N/2} \quad \mathbf{I}_N \quad \mathbf{0}_N)^T\right) + \tilde{\mathbf{R}}_l\left(\mathbf{1}_{N_r} \otimes (\mathbf{0}_{N/2} \quad \mathbf{0}_N \quad \mathbf{I}_N)^T\right) \tag{3.19}$$

$$= 2 \cdot diag\left(\mathbf{t}_l \mathbf{F}_N^{-1}\right)\tilde{\mathbf{H}}_L' + \tilde{\mathbf{W}}_l \qquad , N_t \times N_r N$$

where $\mathbf{1}_{N_r}$ stands for an all-one matrix of size N_r, $\tilde{\mathbf{H}}_L'$ is the same as $\tilde{\mathbf{H}}_L$, only with its elements equal to $\tilde{\mathbf{H}}_l'^{xx}$.

Transformation to frequency domain gives

$$\mathbf{X}_l = \tilde{\mathbf{Y}}_l\left(\mathbf{1}_{N_r} \otimes \mathbf{F}_N\right) = 2 \cdot diag\left(\mathbf{t}_l \mathbf{F}_N^{-1}\right)\tilde{\mathbf{H}}_L'\left(\mathbf{1}_{N_r} \otimes \mathbf{F}_N\right) + \tilde{\mathbf{W}}_l\left(\mathbf{1}_{N_r} \otimes \mathbf{F}_N\right) \tag{3.20}$$

$$= 2 \cdot diag(\mathbf{t}_l)\mathbf{H}_L + \mathbf{W}_l \qquad , N_t \times N_r N$$

with $\mathbf{H}_L$ the same structure as $\tilde{\mathbf{H}}_L$, only with its elements equal to $\mathbf{H}_l^{xx}$.

The incomplete channel estimation matrix is found by demodulation

$$\mathbf{H}_{est,l} = \frac{1}{2} diag\left(\mathbf{t}_l^*\right)\mathbf{X}_L = \mathbf{H}_l + \frac{1}{2} diag\left(\mathbf{t}_l^*\right)\mathbf{W}_L \qquad , N_t \times N_r N \tag{3.21}$$

with $\mathbf{L} = \text{diag}(\mathbf{l})$

To find the complete channel estimations different operations need to be performed on the incomplete channel estimations depending on the implementation.

If the orthogonality rule in (2.9) is used, only the subcarriers corresponding to the ones are estimated. However the unknown subcarriers can be found through interpolation of the known subcarriers. This gives though rise to interpolation errors, but when the channel coherence bandwidth is large enough or equivalently if the time delay spread is small enough (smaller than $\lfloor N_{sc} / N_t \rfloor$ channel taps) the interpolation errors in general will be small.

Next three interpolation methods are described that can be used [12]. In each method H_n stands for the nth channel coefficient, N_t denotes the interpolation interval and x stands for the interpolation step inside each interpolation interval.

Linear interpolation:

$$H_{n+x} = H_n + xA \qquad \text{with} \qquad A = \frac{H_{n+N_t} - H_n}{N_t} \tag{3.22}$$

which requires $N_t N_r$ complex additions + $2N_t N_r$ real multiplications per interpolation step x and requires $N_t N_r$ complex addition + $2N_t N_r$ real multiplications per interpolation interval N_t.

Quadratic interpolation:

$$H_{n+x} = H_n + xB + x^2 C \qquad \text{with} \quad B = \frac{H_{n+N_t} - H_{n-N_t}}{2N_t}, \quad C = \frac{H_{n+N_t} - 2H_n + H_{n-N_t}}{2N_t^2} \tag{3.23}$$

which requires $2N_tN_r$ complex additions + $4N_tN_r$ real multiplications per interpolation step x and requires $3N_tN_r$ complex additions + $6N_tN_r$ real multiplications per interpolation interval N_t.

Cubic interpolation:

$$H_{n+x} = H_n + xD + x^2 E + x^3 F \quad \text{with} \quad D = \frac{-H_{n+2N_t} + 6H_{n+N_t} - 3H_n + 2H_{n-N_t}}{6N_t}, \quad E = \frac{H_{n+N_t} - 2H_n + H_{n-N_t}}{2N_t^2}, \quad F = \frac{H_{n+2N_t} - 3H_{n+N_t} + 3H_n - H_{n-N_t}}{6N_t^3} \tag{3.24}$$

which requires $3N_tN_r$ complex additions + $6N_tN_r$ real multiplications per interpolation step x and $8N_tN_r$ complex additions + $18N_tN_r$ real multiplications per interpolation interval N_t.

If the orthogonality rule in (2.10) or (2.17) is used, the incomplete channel estimation consists out of a mixture of channel estimations. They can be separated using the following interpolation method

$$H_n = \frac{N_t - N_t + 1}{N_t^2} H_{n-N_t+1} + \ldots + \frac{N_t}{N_t^2} H_n + \ldots + \frac{N_t - N_t + 1}{N_t^2} H_{n+N_t-1}. \tag{3.25}$$

which requires $2(N_r\text{-}1)N_tN_r$ complex additions + $2(N_r\text{-}1)N_tN_r$+N_tN_r real multiplications per estimated subcarrier.

Note: All channel estimations are done in frequency domain as channel estimation in time domain gave far worse performance.

Intentionally Blank
KMM

4 Problems & Solutions

A couple of problems should be addressed when the orthogonal channel estimation techniques are used. The first problem concerns the subcarriers at the edge of the spectrum and the subcarriers near the DC subcarrier. The second problem concerns a timing offset in the signal at the receiver.

4.1 Edge Subcarriers and DC Subcarrier

The problem with the subcarriers at the edge of the spectrum is that these subcarriers only have neighbour subcarriers at a single side. This gives problems when a subcarrier at the edge needs to be estimated through some sort of interpolation as has been described in the previous Chapter, because the interpolation methods need subcarriers at either side of the to be estimated subcarrier. As this is not the case the subcarriers will be estimated using extrapolation instead of interpolation. The effect of this will be bigger estimation errors at the edges of the spectrum. The MSE of the subcarriers at the edges is bigger than for the other subcarriers, as can be seen in Figure 4.

Another problem is the absence of the DC subcarrier. This leads to a larger interpolation interval for the subcarriers near the DC subcarrier, resulting in a bigger interpolation error for these subcarriers. This effect is also illustrated in Figure 4.

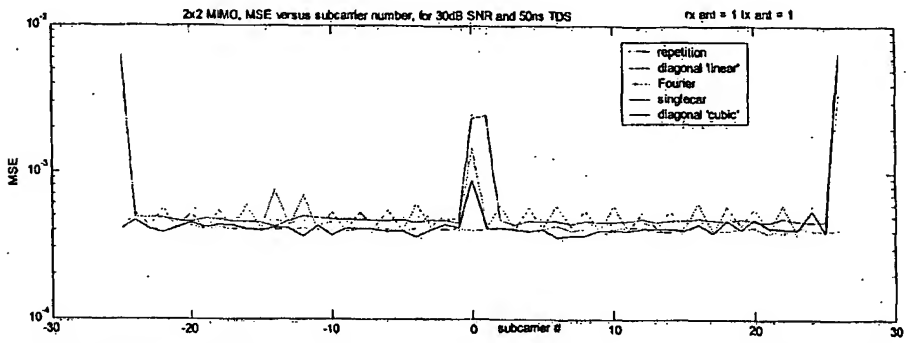

Figure 4: MSE per subcarrier for the channel estimation corresponding to receive antenna 1 and transmit antenna 1 in the case of 2x2 MIMO.

A possible way to overcome the problem of the edge subcarriers is the introduction of additional subcarriers at the spectrum's edges. For a 2x2 MIMO-OFDM system two additional subcarriers are needed, one on each side. For a 3x3 MIMO-OFDM system four extra subcarriers are needed, two on each side. However the addition of extra subcarriers results in a larger overall spectrum and one should take care that the 802.11a transmit spectral mask is not violated. Therefore the PSD of the training sequence is looked at, to be able to see if it still fulfils the transmit spectral mask. To have a realistic transmit spectrum the transmit filter and the power amplifier should be taken into account.

The transmit filter is taken from the Emerald requirements document [14]. The filter is specified as 5th order Butterworth filter, with a cut-off frequency of 13 MHz. The pole locations are as follows

$$\begin{aligned} &p1, p2 = -8.85 \cdot 10^6 \pm j8.92 \cdot 10^6 \\ &p3, p4 = -4.35 \cdot 10^6 \pm j13.00 \cdot 10^6 \\ &p5 = -11.655 \cdot 10^6 . \end{aligned} \tag{4.1}$$

The power amplifier (PA) is modelled by a Rapp's model as described in [13], which represents the AM-AM transfer function of the PA. The specific transfer function of the RFS P2010 amplifier can be written as

$$f(x) = \frac{x}{n\left(1 + (gx)^{2p}\right)^{1/(2p)}} \tag{4.2}$$

where x is the input signal amplitude, g is set to 29.8538, p is set to 1.8 and n is a normalization factor. The backoff of the PA is defined as

$$\text{Backoff} = \frac{\text{power @ 1dB compression point}}{\text{average output power}} \tag{4.3}$$

and is set to 3.5 dB, which is the lowest backoff value used in [13] and therefore gives the highest distortion to the spectrum.

The PSDs of the training sequences including the effects of the transmit filter and PA are shown in Figure 5. The red curve represents the IEEE 802.11a transmit spectrum mask, the green curve represents the PSD of the transmit filter and the yellow curve represents the PSD of the receive filter. Furthermore the blue, cyan and magenta curve represent the PSD of the training sequences, where the cyan one matches the original 802.11a training sequence, the magenta matches the diagonal training sequence as defined in (2.9) and the Fourier training sequence as defined in (2.10) and the blue one matches the single carrier training sequence as defined in (2.17). Each of the training sequences is extended with four extra subcarriers. As can be seen from Figure 5 the PSDs of the training sequences still fulfil the transmit spectral mask requirements, when extended with four additional subcarriers.

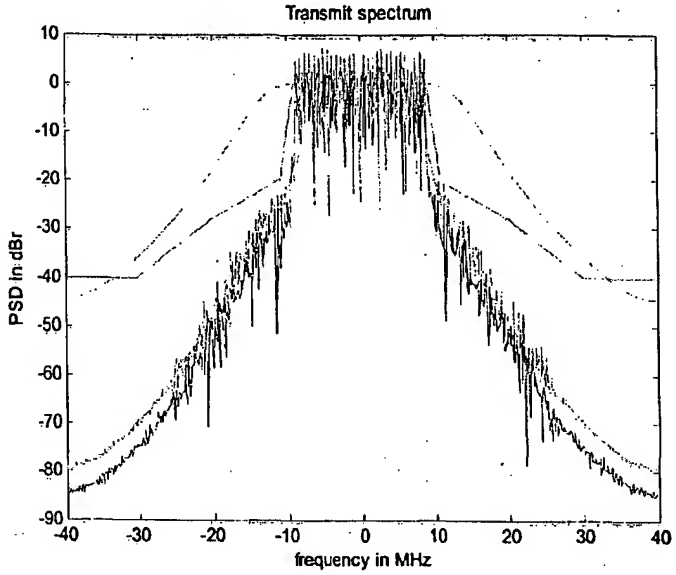

Figure 5: Transmit spectrum of the filtered and PA distorted training sequences

From this it can be concluded that the extension with extra subcarriers at the edges is allowed and is in line with the IEEE 802.11a specifications. So at the transmit side there are no problems foreseen, however the impact on the receive side of the system will be bigger. There a steep receive filter is implemented, mainly to suppress the adjacent channels by a certain level. This filter has its cut-off frequency at about 8.5 MHz, which is lower than the highest subcarrier frequency (8.75 MHz) when four extra subcarriers are added. This means that at the receiver side these subcarriers are weakened by the receive filter. Though these subcarriers are needed to eliminate the extrapolation effects in the channel estimation and therefore need to be in good shape. Consequently the receive filter should be redesigned with increased cut-off frequency. Maybe meaning that the order of the filter needs to be increased too, because the outer-bands still need to be suppressed in the same way.

The MSE per subcarrier is shown in Figure 6 in the case extra subcarriers are applied to the different training sequences. As can be seen the larger MSE at the side subcarriers has disappeared. The larger MSE at the subcarriers near DC still remains, as the addition of extra subcarriers does not benefit these subcarriers. This degradation can unfortunately not be coped with. Finally it can be seen that the average MSE has increased slightly because the total transmit power needs to stay the same in case additional subcarriers are transmitted.

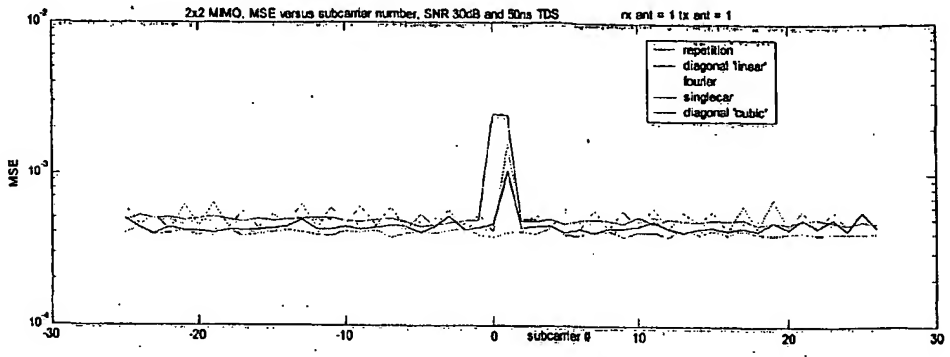

Figure 6: MSE per subcarrier for the channel estimation corresponding to receive antenna 1 and transmit antenna 1 in the case of 2x2 MIMO with addition of extra subcarriers.

4.2 Timing Offset

This section looks at the effect of a timing offset on the different channel estimations techniques. A timing offset causes an incremental phase shift in frequency domain. As a result the training sequences after demodulation in frequency domain loose their orthogonal quality, except for one. This is the diagonal training sequence given in (2.9) when interpolation is separately done for the amplitude and phase.

The loss of orthogonality is illustrated in Figure 7. At a certain point also the diagonal training sequence starts to degrade very rapidly. This effect can be contributed to the wrapping of the phase response of demodulated training sequence. A wrapping of the phase between two successive training subcarriers leads to wrong phase interpolation of the to be estimated subcarrier(s).

With a larger number of antennas the interpolation intervals become larger as well, which means that the effect of phase jumps shows off earlier as seen in Figure 7. Furthermore is can be seen that with more antennas the MSE is larger in general, as a results of the larger interpolation interval, which gives rise to larger interpolation errors.

Finally it can also be seen that with increasing delay spread the MSE of the channel estimation is larger in general and additionally deteriorates faster too. The larger overall estimation error can be contributed to the larger variation of the channel frequency response with increasing delay spread, causing bigger interpolation errors.

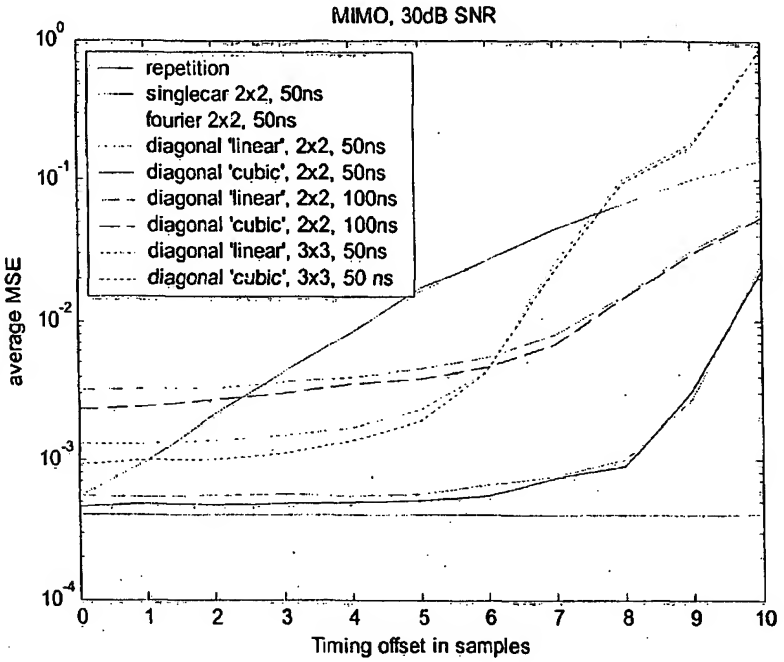

Figure 7: Influence of timing offset on the different channel estimation techniques

Concluding it can be said that the diagonal training sequence designed for a 2x2 MIMO system with 50ns time delay spread can cope with timing offsets up to about 6 samples without additional degradation. With increasing delay spread or with a larger antenna configuration the MSE of the channel estimation increases and the robustness against timing offset decreases. The repetition of 802.11a training sequences in time can handle every number of timing offset samples as long as the guard interval is not exceeded.

Intentionally Blank
KMM

5 PAP-ratio

An important feature of the 11a long training sequences is the low Peak-to-Average Power (PAP) ratio. This minimizes the effect of non-linearity of the PA and prevents clipping in the receiver's ADs. This section looks at the PAP ratios of the original 11a training sequence and the diagonally loaded training sequences for two or three transmit antennas and with zero, two or four additional subcarriers.

The PAP ratios for these training sequences are given in Appendix A. The training sequences with the lowest PAP ratios are listed in a red box. Preferably the training sequence with lowest PAP ratio is used.

Intentionally Blank

6 Backwards Compatibility & Scalability

In wireless communication systems it is very important to be able to adapt your system to the quality of the channel. The channel quality is an ever-changing variable and the communication system needs to optimise itself to that. Furthermore, in general it is important to be backwards compatible with previous standards or equivalently with former systems.

This Chapter looks into the possibilities of scaling a MIMO system to the optimum configuration and whether a MIMO system can be made backwards compatible. To be more specific, with scaling is meant the ability to vary the antenna configuration, the modulation scheme and the coding rate of a MIMO system. Backwards compatibility means two things, first of all a MIMO systems need to be able to support the current standards and secondly an 802.11a system needs to be able to defer for the duration of a MIMO transmission. To comply with the second objective for backwards compatibility an 802.11a system needs to know the exact length of a MIMO transmission.

The length of an 11a transmission can be found in the header its SIGNAL-field. A MIMO transmission will need to have a similar field to address the transmission parameters. An 11a system needs then to be able to detect and decode this field in a MIMO transmission.

6.1 Repeated training

A MIMO system that would use the 802.11a long training sequences repeated on the different transmit antennas in time could easily scale back to a one-antenna configuration and thus satisfies the first backwards compatibility objective.

To comply with the second objective for backwards compatibility this MIMO system requires the transmission of the 11a SIGNAL-field after the long training sequences of the first-in-time antenna. An 11a system is namely expecting the SIGNAL-field after the first two long training sequences. Furthermore the SIGNAL-field needs to be exactly the same as for an 11a system for an 11a system to detect and decode it. The length information in the SIGNAL-field of a MIMO transmission will have to include the length of the additional long training sequences. In this way the 11a system is able to defer for the exact duration of the MIMO transmission. A MIMO receiver will have to subtract the length of the additional long training sequences to get to the right length of the data.

When a MIMO system is scalable in the number of antennas then the MIMO receiver needs to be able to retrieve the number of transmit antennas on forehand, because it needs to know the amount of training still following. Potentially, this information can be stored in the SIGNAL-field succeeding the first long training sequences. However the SIGNAL-field as stated before needs to be kept the same as defined in the 802.11a standard for backwards compatibility. The SIGNAL-field as defined in [11] has only one redundant bit, which is reserved for future use. This bit is available and can be used to specify some antenna information. Though it concerns only a single bit and with one bit it is just possible to discriminate between a SISO and a MIMO system,

but it cannot additionally specify the number of antennas used. To overcome this problem a second SIGNAL-field can be inserted after the second long training sequences, adding up to the overhead, but making 24 bits available to specify additional functionality. The overall preamble structure would then look as in Figure 8.

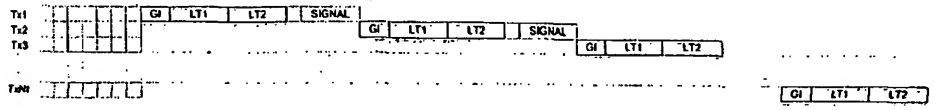

Figure 8: Structure of the preamble

6.2 Diagonally loaded training

A MIMO system, which uses diagonally loaded long training symbols can satisfy the first backwards compatibility constraint by diagonally loading the rest of the header and the data symbols on the different transmit antennas as well. In this case the 802.11a receiver is able to interpret it as a normal OFDM frame. For example for 3 transmitters this would look like as in (6.1) when all ones are transmitted. In this case the receiver would just see the received signal as the channel coefficients belonging to a single channel, even though the different channel coefficients belong to different actual channel realisations.

$$\begin{matrix} T_x^1 \\ T_x^2 \\ T_x^3 \end{matrix}\begin{bmatrix} 1 & 0 & 0 & 1 & 0 & 0 & 1 & \cdots & 0 & 0 & 1 \\ 0 & 1 & 0 & 0 & 1 & 0 & 0 & \cdots & 1 & 0 & 0 \\ 0 & 0 & 1 & 0 & 0 & 1 & 0 & \cdots & 0 & 1 & 0 \end{bmatrix} \tag{6.1}$$

$$R_x\begin{bmatrix} H_1^1 & H_2^2 & H_3^3 & H_4^1 & H_5^2 & H_6^3 & H_7^1 & \cdots & H_{50}^2 & H_{51}^3 & H_{52}^1 \end{bmatrix}$$

Above H_n^t represents the channel coefficient belonging to the n-th subcarrier and the t-th transmitter.

The second compatibility objective can be satisfied when only the SIGNAL-field in the header is diagonally loaded just as the long training sequences. This gives an 11a system the ability to read the SIGNAL-field and therefore able to extract the duration of the transmission. As an 11a system is unable to receive a MIMO transmission it will defer for the duration of the packet. In order to make this work the LENGTH-field in the SIGNAL-field then needs to be aligned with the duration of the transmission. And from that a MIMO system needs to determine the actual length of the packet in bytes. If the length at the transmitter is defined to be in line with number of OFDM symbols in a MIMO case, then there is still some freedom left. Additionally it can specify the number of bytes in the final data OFDM symbol, which inherently specifies the number of padding bits in this symbol. However a MIMO transmission can also contain padding symbols. These symbols cannot be extracted from the LENGTH and RATE-field and should thus be additionally specified.

A MIMO system based on the diagonally loaded training sequences is scalable if it knows the number of transmit antennas on forehand, just as in the repetition training case. Since the number of transmit antennas tells the MIMO receiver, which channel

coefficient belongs to which transmit antenna. The example for 2 transmitters and 3 receivers set up is given in (6.2). As soon as the receiver knows the transmitter's antenna configuration it can reorder the coefficients and estimate the corresponding channels.

$$\begin{matrix} T_x^1 \\ T_x^2 \end{matrix}\begin{bmatrix} 1 & 0 & 1 & 0 & 1 & 0 & 1 & \cdots & 0 & 1 & 0 \\ 0 & 1 & 0 & 1 & 0 & 1 & 0 & \cdots & 1 & 0 & 1 \end{bmatrix}$$

$$\mathrm{R}_x^1\begin{bmatrix} H_1^1 & 0 & 0 & H_4^2 & 0 & 0 & H_7^1 & \cdots & 0 & 0 & H_{52}^2 \\ 0 & H_2^2 & 0 & 0 & H_5^1 & 0 & 0 & \cdots & H_{50}^2 & 0 & 0 \\ 0 & 0 & H_3^1 & 0 & 0 & H_6^2 & 0 & \cdots & 0 & H_{51}^1 & 0 \end{bmatrix} \quad (6.2)$$

A diagonally loaded SIGNAL-field can be detected and decoded without knowing the number of transmit antennas. The SIGNAL-field will be even of better quality than the receive data, because every receive antenna receives the same data and this can be combined in an MRC way. However there is still the need for additional specification in the SIGNAL-field. Since the receiver has to know the number of transmit antennas and furthermore need to know the number of OFDM padding symbols.

Additional information can be included in the SIGNAL-field with the use of extra subcarriers just as in the long training sequences' case. For a 2x2 MIMO system 2 additional subcarriers are needed and for a 3x3 MIMO system 4 additional subcarriers are needed, to be able to sufficiently estimate the subcarriers at the edge of the spectrum. Two extra subcarriers result in two extra available bits and even two more subcarriers mean two more bits.

The reserved bit in the SIGNAL-field is used to specify a SISO or a MIMO system. With one extra bit, two and three transmit antennas can be distinct from each other. Another bit can be used to specify the number of OFDM padding symbols, one or two for three transmitters. As these two extra bits cannot be encoded with the original SIGNAL-field, they are less robust than the other SIGNAL-field bits. The two remaining bits can then be used to add extra robustness. A one-error correcting block code can easily be designed. The two remaining bits could also be used for additional specification, needed when a higher order MIMO system is considered. It is also good to note that when a similar frame structure is adopted for MIMO as for IEEE 802.11a/g, more information can be stored in the reserved bits of the SERVICE-field.

Concluding it can be said that with diagonally loaded training sequences it is possible to be backwards compatible and scalable if the SIGNAL-field is diagonally loaded as well and when additional information is included. The overall preamble would then look like Figure 9.

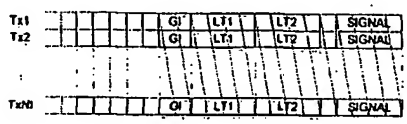

Figure 9: Structure of preamble

Finally it is good to note that a positive property of the diagonally loaded SIGNAL-field is the fact that it actually serves as the third long training symbol. Since after decoding and demodulation the exact bits of the SIGNAL-field are known and can then be used to train the channel. It should though be taken into account that the decoding of the SIGNAL-field takes time and increases the latency when used for channel estimation. When latency becomes a problem a first channel estimate can be based on the two long training symbols and can be updated afterwards. Furthermore when backwards compatibility and scalability are not of importance, the SIGNAL-field can be instead shift-diagonally loaded, as it does not need to serve frequency-offset estimation.

Additionally be aware of the fact that when the training symbols are repeated on each antenna they all should be able to transmit full power. While with diagonally loaded training symbols they only need to be able to transmit power/Nt, resulting in cheaper PAs. Furthermore it is possible to transmit with more power as the limiting factor most of the times is not the output power specified in the regulations, but the PA itself that cannot achieve these high output powers without distortion, which is a direct result of the technology where the PA is designed in.

7 Performance Analysis

This section looks into several performance measures of the different channel estimation algorithms. First of all the MSE of the channel estimation versus the SNR for certain TDS and antenna configurations is looked at. Secondly the effect of TDS on the SNR at which the MSE of the channel estimation for the diagonally loaded training sequence equals the MSE of the channel estimation for the repeated training sequences is considered. Finally the PER performance of a 2x2 MIMO system with channel estimation is considered.

The channel implementation is an exponentially Rayleigh fading channel with a length 10 times the rms time delay spread for every independent channel in space. Furthermore the channel is not normalised to have instantaneous power, which is different from the analysis done for the 802.11a system. Meaning that the channels undergo a combination of selective and flat fading.

7.1 MSE versus SNR

The simulations carried out in this subsection are done with a fixed TDS and varying SNR. For a 2x2 MIMO system and a 3x3 MIMO system the average MSE over the subcarriers of the channel estimation is recorded for the varying SNR over 200 different channel representations. Figure 10 shows the results of the various channel estimation techniques for several TDS. The enlarged replicas can be found in Appendix B.

The figures show that after a certain SNR the performance of the orthogonal channel estimations goes down and this continues until a certain error floor is reached. This can be subscribed to interpolation. At a certain SNR point the interpolation error becomes bigger than the noise error and this is the point where the orthogonal channel estimations loose performance compared to the sequential channel estimations. It can be seen that at higher TDS this effect occurs at lower SNR than for lower TDS, obviously because the channel is more selective at higher TDS. Furthermore this effect is visible at lower SNR for higher order MIMO systems, caused by the increase of interpolation steps.

It can be seen that the channel estimations with the diagonally loaded training sequences outperform the other orthogonal channel estimation techniques at higher SNR. This is especially true with cubic interpolation. The channel estimations based on the Fourier training and the single carrier training degrade earlier than the channel estimation based on the diagonally loaded training. This can be contributed to the fact that these channel estimations have worse estimates of the subcarriers near the 0 Hz subcarrier as depicted in Figure 6.

Finally the dashed curves in the figures represent the case where three (so including the SIGNAL-field) instead of two long training sequences are used for channel estimation. The performance at low SNR increases because the noise is averaged out more. The error floor will stay the same while it is determined by the interpolation errors and adding an extra training symbol does not make interpolation more accurate. Logically the point where the MSE of the orthogonal channel estimation crosses the

MSE of the sequential channel estimation with less training shifts to higher SNR. It is therefore always better to use three instead of two long training symbols.

As the interpolation error becomes dominant above a certain SNR for a specific TDS it is interesting to look at a shift-diagonally loaded third long training symbol (actually the SIGNAL-field), keeping in mind that such a solution is not backwards compatible anymore. Though this should lead to a more reliable channel estimate, while in this case some knowledge of the to be interpolated subcarriers is available. In a 2x2 MIMO system all subcarriers can be estimated without interpolation and in a 3x3 MIMO system only one out of the three subcarriers needs to be interpolated. However the subcarriers estimated using the third long training symbol do not have the additional gain in SNR and therefore will be worse in general. Alternatively, through separately interpolating the first added two long training symbols and the third long training symbol a gain in SNR over all subcarriers is achieved and furthermore the interpolation error is decreased. This result is depicted as the orange dashed line in Figure 10. For a 2x2 MIMO system with linear interpolation this is mathematically shown in Appendix C.

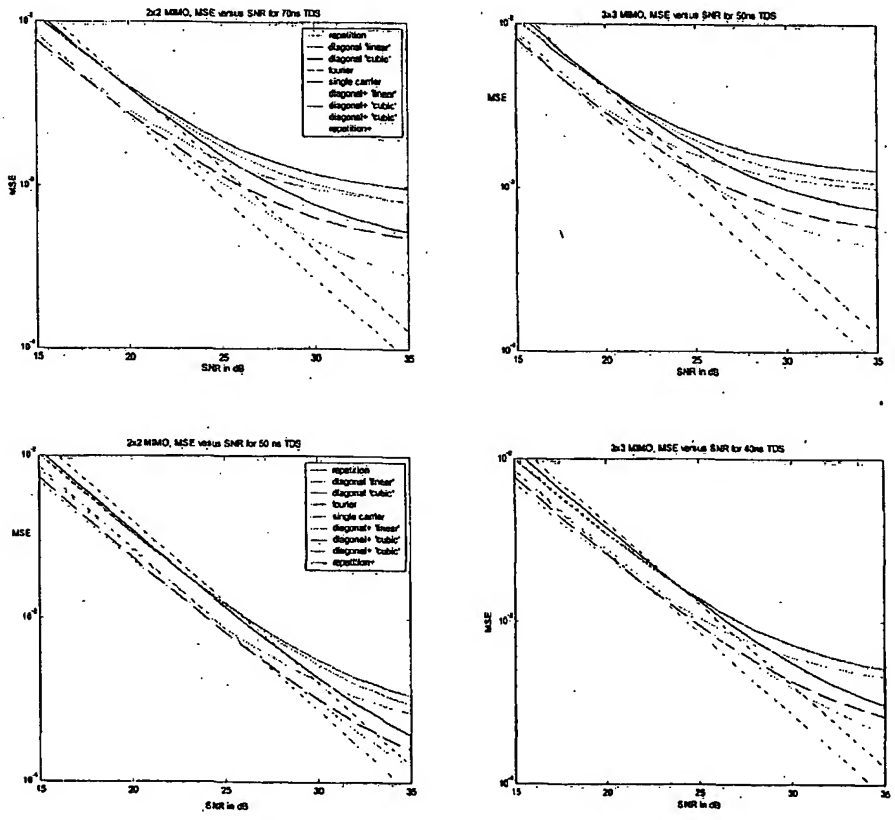

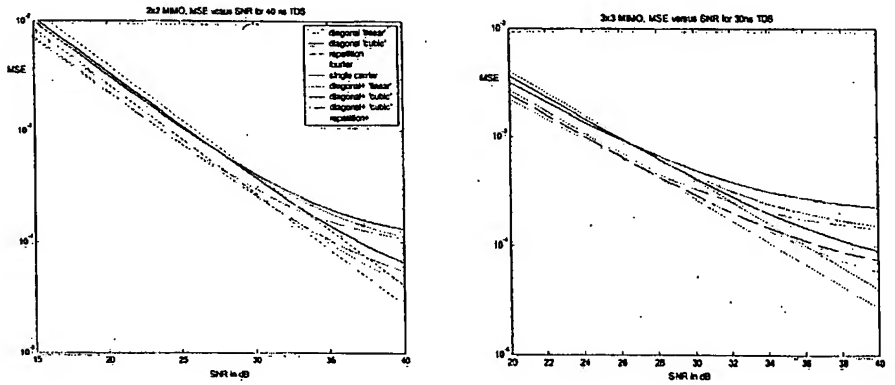

Figure 10: MSE of the various channel estimation techniques versus SNR for different MIMO set-ups and several TDS.

7.2 TDS versus SNR

From the previous subsection it became clear that the TDS has a big influence on the MSE of the orthogonal channel estimations. It is therefore interesting to study this effect a bit closer.

Figure 11 and Figure 12 show the SNR at which the MSE of the orthogonal channel estimations intersects the MSE of the sequential channel estimations for a range of TDS and two different antenna configurations. It actually shows the SNR at which a certain amount of TDS can still be handled without loss in channel estimation accuracy compared to the sequential channel estimation. The solid lines represent the case with two long training symbols and the dashed lines represent the case with three long training symbols. Furthermore the blue and green curves represent a 3x3 MIMO system and the pink and black curves represent a 2x2 MIMO system, with respectively linear and cubic interpolation.

Clearly it can be seen that a 3x3 MIMO system can handle less TDS for a given SNR than a 2x2 MIMO system as was already clear from the previous subsection. Additionally it can be seen that at higher TDS the linear interpolation becomes a bit better than the cubic interpolation. This can be explained from the fact that cubic interpolation takes into account more neighbour subcarriers to estimate the unknown subcarriers in between and with higher TDS the channel is more frequency selective and therefore neighbour subcarriers are not as correlated as with lower TDS.

The general observation from Figure 11 and Figure 12 is the higher the SNR the less TDS can be tolerated. High SNRs are needed to be able to successfully receive the highest rates. From the indoor Raytracing figures for typical office environments in Appendix D it can be concluded that close to the source the TDS is low and the SNR is high, moving away from the source increases the TDS and decreases SNR. This is exactly in line with the TDS behaviour of the channel estimation.

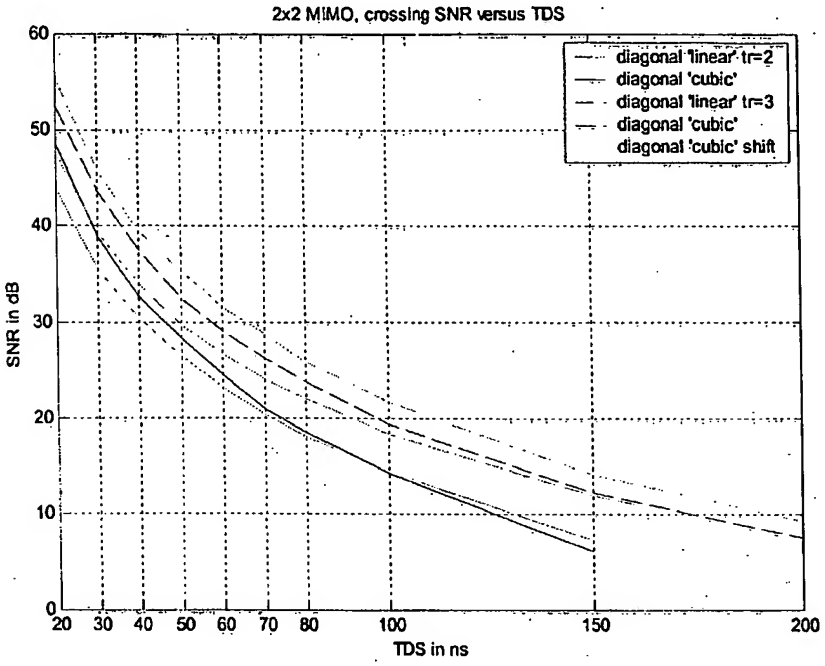

Figure 11: SNR of the MSE cross-points versus TDS for a 2x2 MIMO system

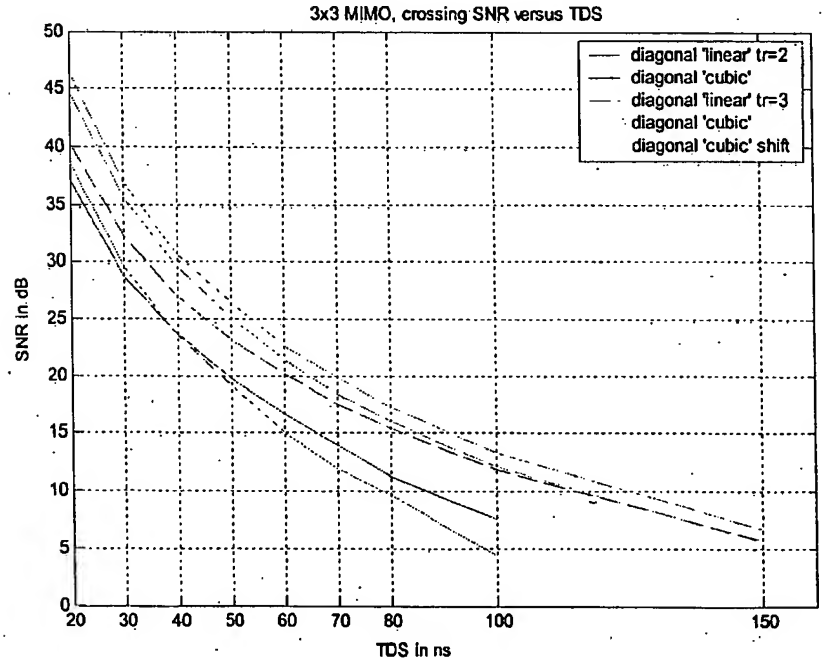

Figure 12: SNR of the MSE cross-points versus TDS for a 3x3 MIMO system

7.3 PER versus SNR

This section looks at the PER performance of the orthogonal channel estimation with diagonally loaded training sequences compared to the sequential channel estimation. From the previous subsection the SNR range of interest can be determined for a certain TDS. Taking a TDS of 50ns as a reference it can be concluded from Figure 11 that the interesting SNR range is between 25 and 30 dB as the MSE of the orthogonal channel estimation intersects there with the MSE of the sequential channel estimation. This is about the SNR range that is achievable in real-life systems when implementation loss and other imperfections are taken into account.

Figure 13 shows for the given configuration the PER of a 2x2 MIMO system for orthogonal and sequential channel estimations. The simulations are carried out over 100,000 packets. It can be seen that the orthogonal channel estimation curves indeed cross the sequential channel estimation one as expected from Figure 11. It is shown again that channel estimation with three training symbols of which one is shift-diagonally loaded leads to the best overall performance. Figure 13 also shows the absolute error between the ideal channel and the different channel estimations.

Figure 14 shows the same results as Figure 13 but now for 1000 bytes packet and soft decision detection algorithm. These simulations are carried out over 10,000 packets to control simulation time. Similar results are seen as before.

Finally Figure 15 gives the results for a 3x3 MIMO system. The simulations are again carried out over 100,000 packets. For 50ns TDS the performance degrades at lower SNR than for a 2x2 system, in agreement with the results in Figure 12.

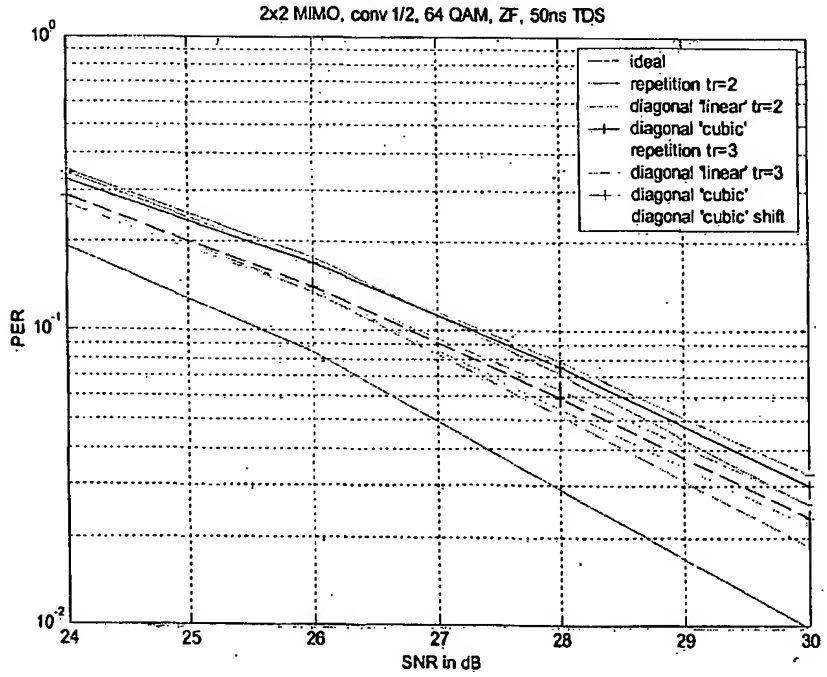

Figure 13: PER versus SNR, for a 2x2 MIMO system with coding rate ½, 64 QAM, 64 bytes packets, Zero-Forcing with hard decision and 50ns TDS.

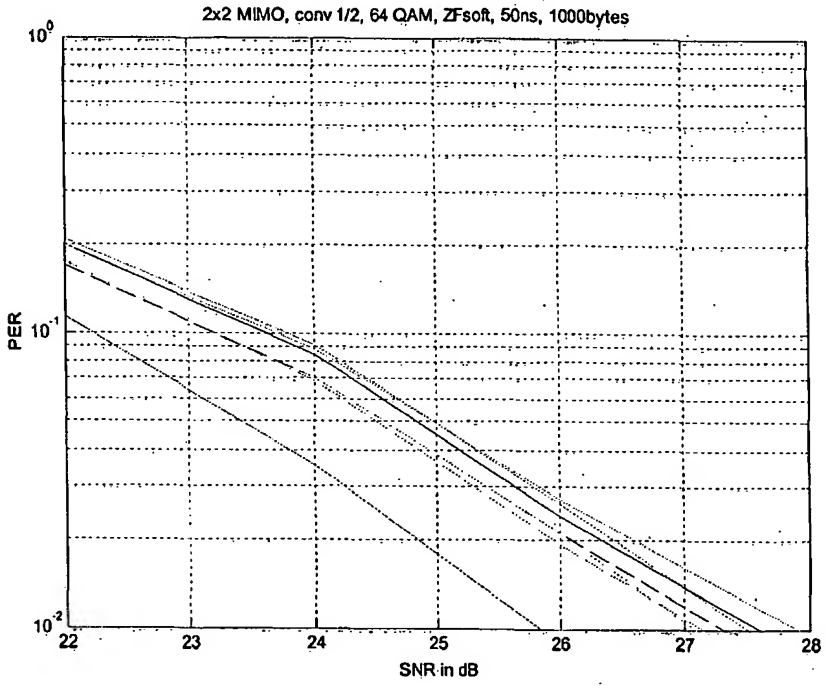

Figure 14: PER versus SNR, for a 2x2 MIMO system with coding rate ½, 64 QAM, 1000 bytes packets, Zero-Forcing with soft decision and 50ns TDS.

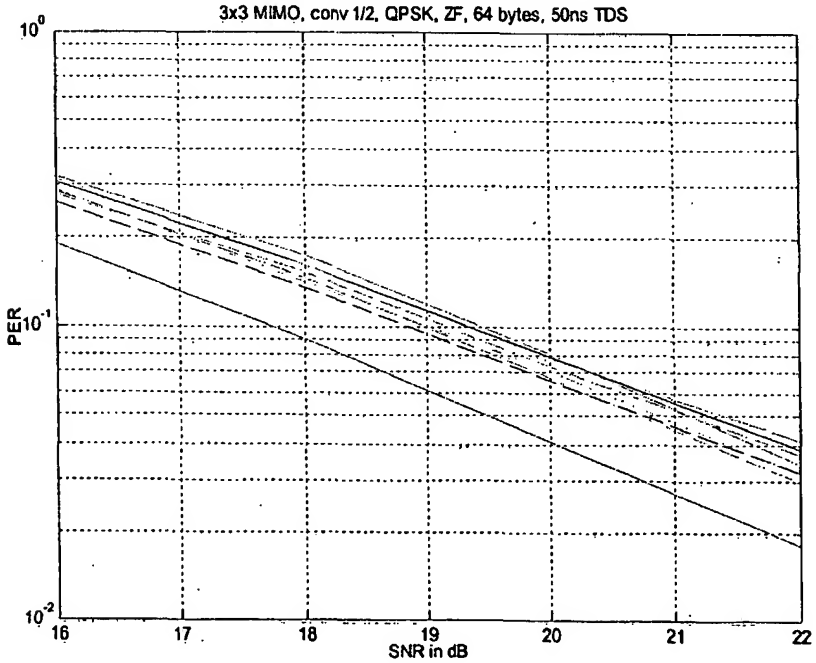

Figure 15: PER versus SNR, for a 3x3 MIMO system with coding rate ½, QPSK, 64 bytes packets, Zero-Forcing with hard decision and 50ns TDS.

8 Conclusions & Recommendations

Several orthogonal channel estimation techniques are studied. All but one is able to handle timing offset till some amount, when phase and amplitude are separately processed. The accompanying training sequence is the diagonally loaded one.

To overcome the inaccuracy of the channel estimation's edge subcarriers extra subcarriers at either side of the spectrum's edge can be added. A 2x2 MIMO system would benefit from 2 additional subcarriers, one at each side. The PAP-ratio is smallest when the extra subcarrier at the left side of the spectrum is set to –1 and the extra subcarrier at the right side is set to 1. A 3x3 MIMO system would benefit additionally with 2 extra subcarriers, four in total and two on each side. The PAP-ratio is smallest when all four extra subcarriers are set to –1.

The diagonally loaded training sequences are backwards compatible and a system based on it can be made backwards compatible and scalable. The SIGNAL-field should as well be diagonally loaded, which creates the important advantage that it can be used as a third long training symbol. Extra information, which is needed in case of a MIMO transmission, can be included in the additional subcarriers at the edges. It is shown that having shift-diagonally loaded training symbols leads to better interpolation, but the disadvantage is that such training is not backwards compatible anymore.

A major advantage, apart from the fact that diagonally loaded training sequences are very time efficient, is the fact that each transmit chain only has to be able to transmit P_{max}/Nt, whereas every transmit chain would need to be able to transmit P_{max} when sequentially transmitting the 802.11a training sequence on every antenna. This could result in cheaper PAs and more total output power, as the output power is PA limited while the regulations allow more output power.

A disadvantage of the orthogonal channel estimation is that it limits the TDS robustness for a given SNR. Exceeding a certain SNR for a specific TDS results in loss of channel estimation accuracy and inherently loss of performance. At 50 ns TDS, 2x2 MIMO channel estimation, using two diagonally loaded long training symbols and a diagonally loaded SIGNAL-field encounters no additional loss till 32 dB of SNR when compared to a SISO system, using only two full training symbols without any interpolation. The loss in performance above a certain SNR for a specific TDS can be assigned to the interpolation error, which then becomes dominant. However in typical indoor environments as small offices and homes the TDS will in general be smaller than 50 ns, especially close to the source and therefore the channel estimation error will be small enough.

Overall it can be said that the orthogonal channel estimation based on diagonally loaded training sequences is feasible up to 3x3 MIMO. Although TDS robustness for a 3x3 MIMO system decreases significantly it will still be satisfying in typical indoor environments. Going to higher order MIMO systems will certainly require additional training. A rule of thumb is one long training symbol per transmit and receive antenna. Thus transmitting 4 diagonally loaded long training sequences instead of 2 could achieve a 4x4 MIMO system.

Intentionally Blank

KMM

9 References, each incorporated by reference herein.

[1] A. v. Zelst, Dissertation on MIMO, to be published.

[2] R. v. Nee, "*Channel training in space division multiplexing systems*", IDR, June 1, 2000, patent pending.

[3] Y. Li, N. Seshadri, S. Ariyavisitakul, "*Channel estimation for OFDM systems with transmitter diversity in mobile wireless channels*", IEEE, Journal on selected areas in communications, vol. 17, No. 3, March 1999.

[4] Y. Li, "*Simplified channel estimation for OFDM systems with multiple transmit antennas*", IEEE, Transactions on wireless communications, Vol. 1, No. 1, January 2002.

[5] E. G. Larsson and J. Li, "*Preamble design for multiple-antenna OFDM-based WLANs with null subcarriers*", IEEE, Signal processing letters, Vol. 8, No. 11, November 2001.

[6] S. B. Slimane, "*Channel estimation for HIPERLAN/2 with transmitter diversity*", IEEE, 2002.

[7] Y. H. You et al., "*Impact of imperfect channel estimation in OFDM-based spatial multiplexing*", IEE, Electronic letters, Vol. 38, No. 24, November 2002.

[8] I. Barhumi, G. Leus and M. Moonen, "*Optimal training sequences for channel estimation in MIMO OFDM systems in mobile wireless channels*", IEEE, Seminar on Broadband Communications, 2002.

[9] T. L. Tung et al., "*Channel estimation and adaptive power allocation for performance and capacity improvement of multiple-antenna OFDM systems*", IEEE, Signal Processing Workshop, March 2001.

[10] I. Modonesi, "*Channel estimation in MIMO-OFDM systems*", Internal Agere Systems document.

[11] IEEE Std 802.11a-1999, "*Part 11: Wireless LAN medium access control (MAC) and physical layer (PHY) specification: high-speed physical layer in the 5 GHz band*".

[12] Q. Sun, "*Effect of channel estimation error on MIMO systems and CDMA systems with multiuser detection*", Dissertation, Stanford University, October 2001.

[13] Y. Yuan, "*Clipping in the I and Q transmitter path*", Agere Internal Design Note, No. 105, Rev. B, 23 April, 2002.

[14] Emerald W4160 Product Requirements Document, Rev. 0.5, Agere Internal, 2002.

[15] F. Zadoff, "*Phase shift pulse codes with good periodic correlation properties*", IEEE, December 29, 1961.

[16] R.C. Heimiller, "*Phase shift pulse codes with good periodic correlation properties*", IRE, Transactions on information theory, October, 1961.

[17] G.J. Foschini and M.J. Gans, "*On limits of wireless communications in a fading environment when using multiple antennas*", AT&T-Bell Labs Internal Tech. Memo, Sept. 1995.

[18] G.J. Foschini, "*Layered space-time architecture for wireless communication in a fading environment when using multiple antennas*", Bell Laboratories Technical Journal, Vol. 1, No.2, autumn 1996.

[19] J.H. Winters, J. Salz, R.D. Gitlin, "*The impact of antenna diversity on the capacity of wireless communication systems*", IEEE Trans. on communications, Vol. 42, No. 2, Feb. 1994.

[20] P.W. Wolniansky, G.J. Foschini, G.D. Golden, R.A. Valenzuela, "*V-Blast: An architecture for realizing very high data rates over the rich-scattering wireless channel*", 1998 URSI International Symposium on Signals, Systems, and Electronics, ISSSE 98, Sept. 1998.

[21] A. v. Zelst, M. Sc. Thesis

Appendix A: PAP ratios training sequences

	Extra Bits	Antenna	Max Power	Mean Power	PAP
802.11a	0	1	4.1458	2.0000	2.0729
Diagonal-0	0000	1	4.0101	1.0000	4.0101
		2	3.8462	1.0000	3.8462
	0000	1	2.9518	1.0385	2.8424
		2	2.2940	0.9808	2.3390
		3	2.8269	0.9808	2.8824
Diagonal-2	0110	1	4.4815	1.0000	4.4815
		2	4.4815	1.0000	4.4815
	01-10	1	4.4815	1.0000	4.4815
		2	4.5817	1.0000	4.5817
	0-110	1	3.0000	1.0000	3.0000
		2	4.4815	1.0000	4.4815
	0-1-10	1	3.0000	1.0000	3.0000
		2	4.5817	1.0000	4.5817
Diagonal-4	1111	1	2.9337	1.0179	2.8822
		2	4.3393	1.0179	4.2632
		3	2.7409	0.9643	2.8424
	111-1	1	2.9337	1.0179	2.8822
		2	4.3393	1.0179	4.2632
		3	2.7409	0.9643	2.8424
	11-11	1	3.0600	1.0179	3.0063
		2	4.3393	1.0179	4.2632
		3	2.7409	0.9643	2.8424
	11-1-1	1	3.0600	1.0179	3.0063
		2	4.3393	1.0179	4.2632
		3	2.7409	0.9643	2.8424
	1-111	1	2.9337	1.0179	2.8822
		2	3.0265	1.0179	2.9734
		3	2.7409	0.9643	2.8424
	1-11-1	1	2.9337	1.0179	2.8822
		2	2.7592	1.0179	2.7108
		3	2.7409	0.9643	2.8424
	1-1-11	1	3.0600	1.0179	3.0063
		2	3.0265	1.0179	2.9734
		3	2.7409	0.9643	2.8424
	1-1-1-1	1	3.0600	1.0179	3.0063
		2	2.7592	1.0179	2.7108
		3	2.7409	0.9643	2.8424
	-1111	1	2.6520	1.0179	2.6055
		2	4.3393	1.0179	4.2632
		3	2.7409	0.9643	2.8424
	-111-1	1	2.6520	1.0179	2.6055
		2	4.3393	1.0179	4.2632

		3	2.7409	0.9643	2.8424
	-11-11	1	2.2224	1.0179	2.1834
		2	4.3393	1.0179	4.2632
		3	2.7409	0.9643	2.8424
	-11-1-1	1	2.2224	1.0179	2.1834
		2	4.3393	1.0179	4.2632
		3	2.7409	0.9643	2.8424
	-1-111	1	2.4626	1.0179	2.6055
		2	2.8103	1.0179	2.9734
		3	2.5451	0.9643	2.8424
	-1-11-1	1	2.6520	1.0179	2.6055
		2	2.7592	1.0179	2.7108
		3	2.5451	0.9643	2.8424
	-1-1-11	1	2.2224	1.0179	2.1834
		2	2.8103	1.0179	2.9734
		3	2.5451	0.9643	2.8424
	-1-1-1-1	1	2.2224	1.0179	2.1834
		2	2.7592	1.0179	2.7108
		3	2.5451	0.9643	2.8424

Appendix B: MSE versus SNR

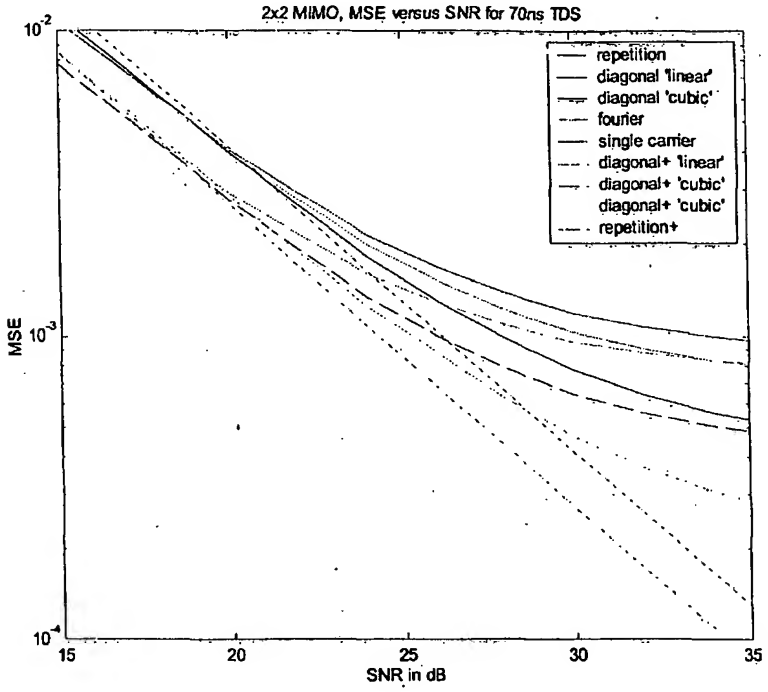

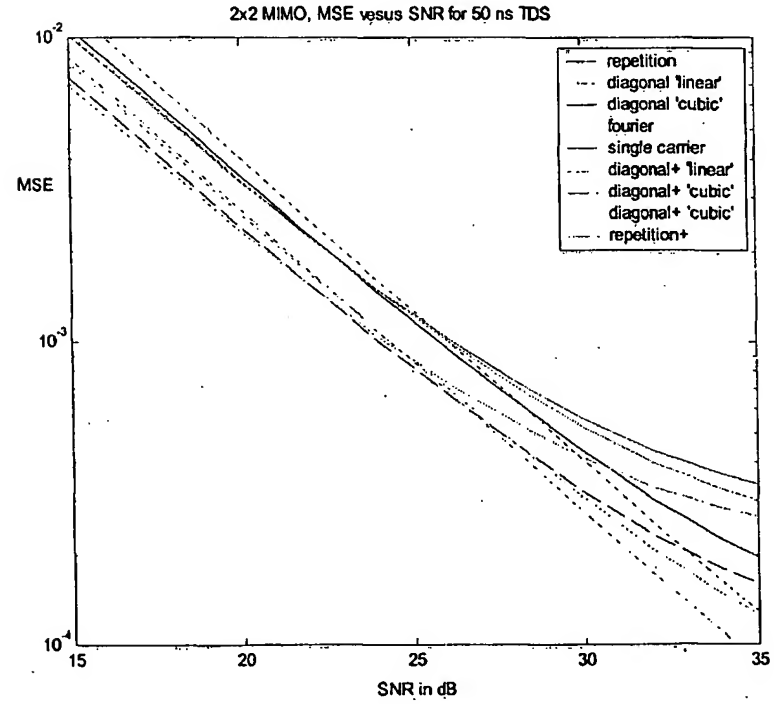

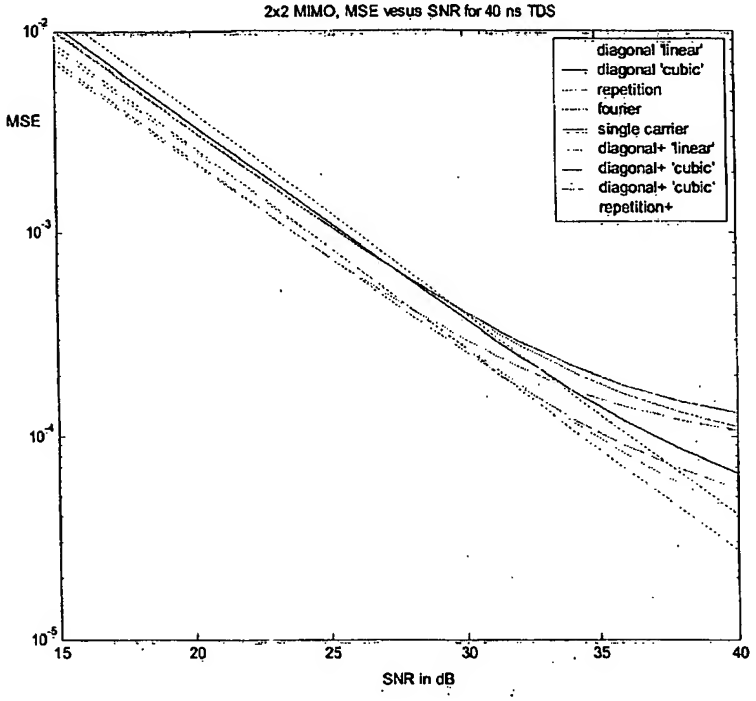
2x2 MIMO, MSE vesus SNR for 40 ns TDS
MSE
SNR in dB
diagonal 'linear'
diagonal 'cubic'
repetition
fourier
single carrier
diagonal+ 'linear'
diagonal+ 'cubic'
diagonal+ 'cubic'
repetition+

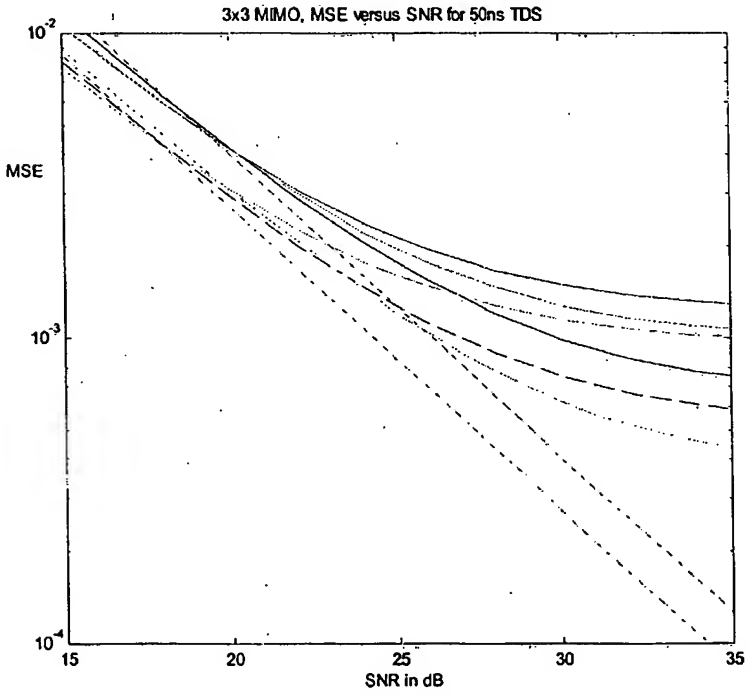
3x3 MIMO, MSE versus SNR for 50ns TDS
MSE
SNR in dB

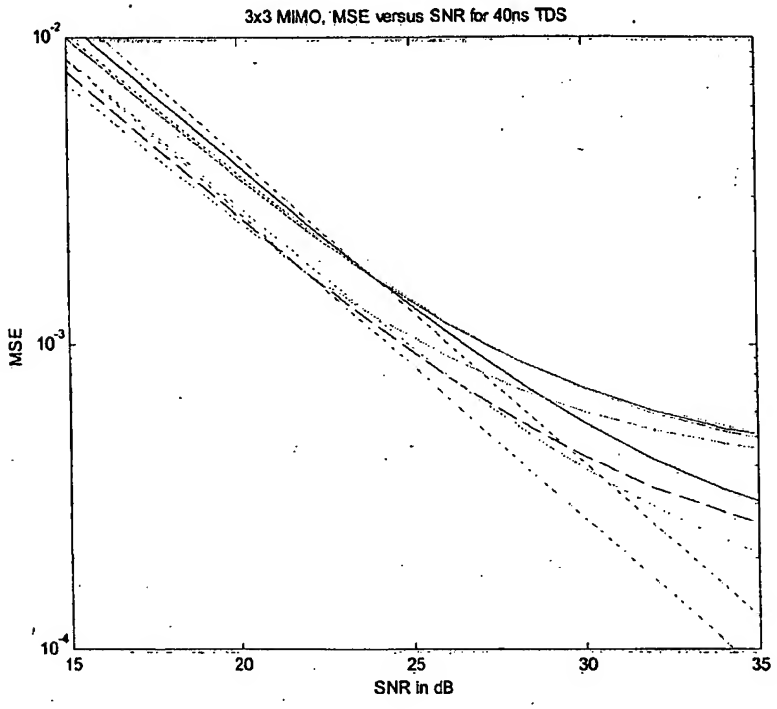
3x3 MIMO, MSE versus SNR for 40ns TDS
MSE
SNR in dB
10^-2
10^-3
10^-4
15
20
25
30
35

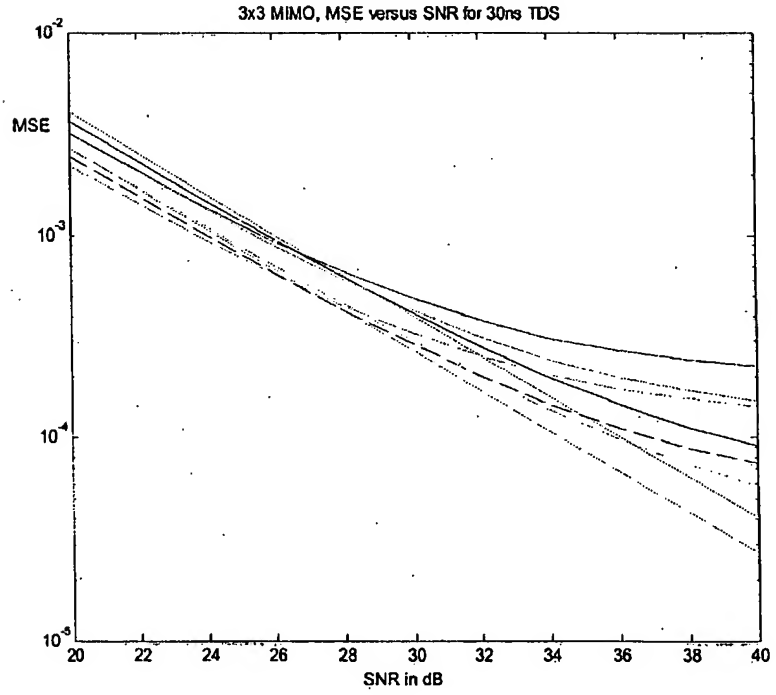
3x3 MIMO, MSE versus SNR for 30ns TDS
MSE
SNR in dB
10^-2
10^-3
10^-4
10^-5
20
22
24
26
28
30
32
34
36
38
40

Appendix C: Effect of Interpolation

Case one: Similar diagonally loaded first and second long training symbol and shift diagonally loaded third long training symbol.

$$\begin{matrix} LT_1 \\ LT_2 \\ LT_3 \end{matrix}\begin{bmatrix} H_x + n_{x,1} & 0 & H_{x+2} + n_{x+2,1} & 0 \\ H_x + n_{x,2} & 0 & H_{x+2} + n_{x+2,2} & 0 \\ 0 & H_{x+1} + n_{x+1,3} & 0 & H_{x+3} + n_{x+3,3} \end{bmatrix}$$

$$\hat{H}_{x+1} = \frac{1}{4}\left\{H_x + \frac{1}{2}\left(n_{x,1} + n_{x,2}\right) + H_{x+2} + \frac{1}{2}\left(n_{x+2,1} + n_{x+2,2}\right)\right\} + \frac{1}{2}\left\{H_{x+1} + n_{x+1,3}\right\}$$

$$\hat{H}_{x+1} = \frac{1}{2}\left\{H_{x+1} + \Delta H_{x+1} + \frac{1}{4}\left(n_{x,1} + n_{x,2} + n_{x+2,1} + n_{x+2,2}\right)\right\} + \frac{1}{2}\left\{H_{x+1} + n_{x+1,3}\right\}.$$

$$\hat{H}_{x+1} = H_{x+1} + \frac{1}{2}\Delta H_{x+1} + \frac{1}{8}\left(n_{x,1} + n_{x,2} + n_{x+2,1} + n_{x+2,2} + 4n_{x+1,3}\right)$$

$$\Rightarrow \sigma^2_{\hat{H}_{x+1}} = \sigma^2_{H_{x+1}} + \frac{1}{4}\sigma^2_{\Delta H_{x+1}} + \frac{5}{16}\sigma^2_n$$

$$\hat{H}_{x+2} = H_{x+2} + \frac{1}{2}\Delta H_{x+2} + \frac{1}{4}\left(n_{x+2,1} + n_{x+2,2} + n_{x+1,3} + n_{x+3,3}\right)$$

$$\Rightarrow \sigma^2_{\hat{H}_{x+2}} = \sigma^2_{H_{x+2}} + \frac{1}{4}\sigma^2_{\Delta H_{x+2}} + \frac{1}{4}\sigma^2_n$$

Case two: Similar diagonally loaded long training sequences

$$\begin{matrix} LT_1 \\ LT_2 \\ LT_3 \end{matrix}\begin{bmatrix} H_x + n_{x,1} & 0 & H_{x+2} + n_{x+2,1} & 0 \\ H_x + n_{x,2} & 0 & H_{x+2} + n_{x+2,2} & 0 \\ H_x + n_{x,3} & 0 & H_{x+2} + n_{x+2,3} & 0 \end{bmatrix}$$

$$\Rightarrow \sigma^2_{\hat{H}_{x+1}} = \sigma^2_{H_{x+1}} + \sigma^2_{\Delta H_{x+1}} + \frac{1}{6}\sigma^2_n$$

$$\Rightarrow \sigma^2_{\hat{H}_{x+2}} = \sigma^2_{H_{x+2}} + \frac{1}{3}\sigma^2_n$$

It can be seen that case one has a smaller and more equally distributed interpolation error compared to case two. This is the reason why channel estimation based on case one gives better results when the interpolation error becomes dominant.

Appendix D: 3D Pincushion Raytracing, 5 Bounces

Received Power

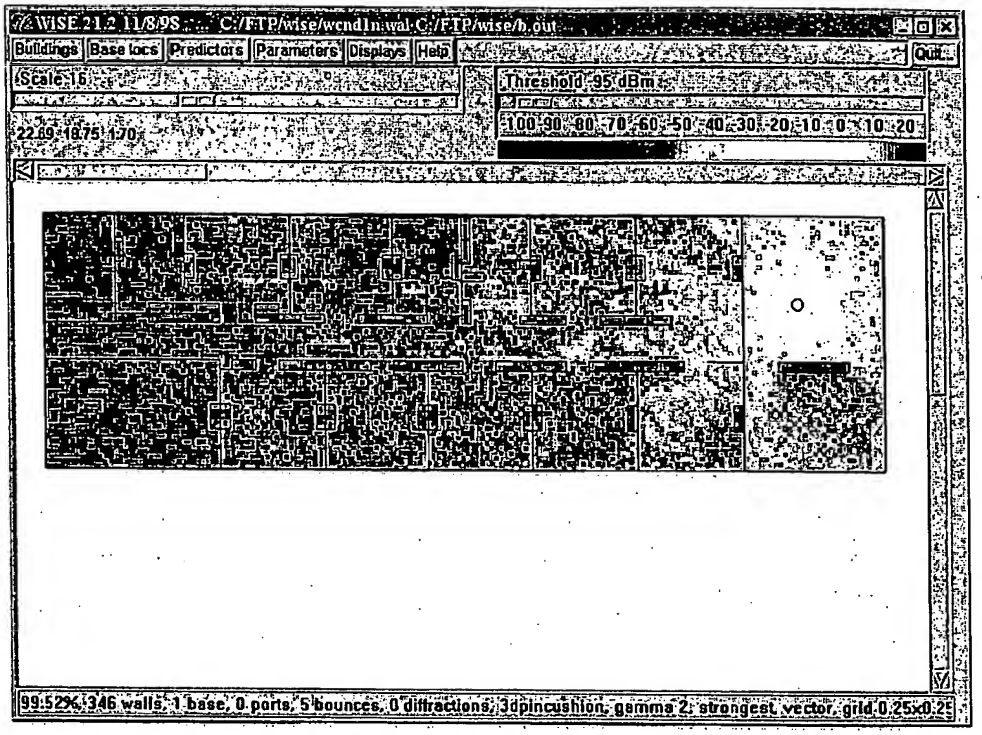

RMS Delay Spread